

MARINE PHYSICAL
LABORATORY

SCRIPPS INSTITUTION OF OCEANOGRAPHY

San Diego, California 92152

AD-A197 630

4

Broadband Spectral Estimation Using the Multiple
Window Method: A Comparison with Classical Techniques

Jean-Marie Tran

MPL TECHNICAL MEMORANDUM 403

MPL-U-16/88

Approved for public release; distribution unlimited.

June 1988

DTIC
ELECTE
S JUL 06 1988 D
SH

CONTENTS

1. Introduction
2. Analysis Description
3. Outline Of The Multiple Window Method
4. Outline Of The Maximum Likelihood Method
5. Ambient Noise Data
6. Averaged Periodogram Estimate
7. Multiple Window Estimate
 - 7.1. Selection Of The Time Bandwidth Product NW
 - 7.2. MW Estimate On 128 Points With NW=2
 - 7.3. MW Estimate On 128 Points With NW=3
 - 7.4. MW Estimate On 576 Points With NW=4
8. Maximum Likelihood Estimate
 - 8.1. Order Selection
 - 8.2. MLM Estimate Of Order 8 On 128 Points
 - 8.3. MLM Estimate Of Order 16 On 128 Points
 - 8.4. MLM Estimate Of Order 32 On 128 Points
 - 8.5. MLM Estimate Of Order 32 On 576 Points
9. Conclusions
10. References



Accession For	
NTIS GRA&I	<input checked="" type="checkbox"/>
DTIC TAB	<input type="checkbox"/>
Unannounced	<input type="checkbox"/>
Justification	<input type="checkbox"/>
By	
Distribution	
Availability	
Avail and/or	
DISC	
A-1	

Broadband Spectral Estimation Using The Multiple Window Method A Comparison With Classical Techniques

Jean-Marie Tran

Marine Physical Laboratory
Scripps Institution Of Oceanography
San Diego, CA 92152



ABSTRACT

The Multiple Window recently introduced by D.J. Thomson is an alternative approach to spectral estimation. Using an orthogonal decomposition of the Discrete Fourier Transform of the data on the prolate spheroidal wave sequences, the power spectrum is estimated by a weighted average of raw spectra obtained from the Fourier transforms of the data windowed by the prolate sequences. This method has the reputation of working well on short data sequences, offering good variance control and a fair resolution. Because the Multiple Window technique combines Fourier transforms with data adaptive weighting, it is compared, in a Monte Carlo simulation, to more conventional spectral estimation methods : the classic averaged Fourier transforms technique and Capon's Maximum Likelihood method. The underlying spectral density to be estimated is of an ARMA process simulating underwater acoustic ambient noise. It is characterized by a moderate dynamic range of 30 dB and can be regarded as a generic spectrum of many applications. The three methods considered here are non parametric, so that no estimator has an unfair advantage. The normalized bias, random and root mean square errors, as well as the statistical distributions, based on 512 realizations of the spectral density, quantify the performance of the three different techniques.

(n/m) ←



1. Introduction

The multiple Window method introduced by Thomson [1,2,3] is a new spectral estimation method that has the reputation of working well on short data sequence, offering good variance control, bias protection and fair resolution.

It is of interest to compare in a Monte Carlo simulation the resolution capabilities and the statistical characteristics of the Multiple Window method with classical methods such as the conventional FFT spectral estimation method and the Maximum Likelihood method.

This simulation focuses on broadband spectral estimation. The reference spectrum, estimated by the various methods, is characteristic of an underwater acoustic ambient noise spectrum between DC and 250 Hz. The main features of ambient noise spectra are a moderate 20 to 30 dB dynamic range, a red part at low frequency and an almost white part at high frequency [4]. This reference spectrum can be regarded as a generic spectrum characteristic of many applications.

After an outline of the analysis, some background material relevant to the Multiple Window method and the Maximum Likelihood method are presented. Then the ARMA process creating the data that simulate the ambient noise is described. Finally, results of the simulation are given and discussed.

2. Analysis Description

The sampling frequency is assumed to be 500 Hz so that the power spectrum lies between DC and 250 Hz. All the results presented on the plots are given in terms of the fractional sampling frequency, between 0 and 0.5 of the Nyquist frequency.

Each spectral estimate is characterized by the following plots :

- (1) the overlaid realizations of the estimated power spectrum
- (2) the mean and envelope of the realizations of the power spectrum
- (3) the normalized random error
- (4) the normalized bias error
- (5) the normalized root mean square error
- (6) the distributions of the estimate at the normalized frequencies : 10/512, 50/512, 200/512 (or 9.76 Hz, 48.8 Hz and 195 Hz), surimposed with fitted Gaussian and chi-square distributions converted in number of observations.

The error estimates allow an overall rating of the different methods. The normalized errors are defined as in [5]. The normalized random error ϵ_r is

$$\epsilon_r = \frac{\sqrt{\text{VAR}(\hat{\Phi})}}{\Phi} \quad (1.1)$$

where VAR is the variance operator, $\hat{\Phi}$ is the power spectral density estimate and Φ is the true underlying spectrum. The normalized bias error ϵ_b is

$$\epsilon_b = \frac{E(\hat{\Phi})}{\Phi} - 1 \quad (1.2)$$

where E is the mean. The root mean square (rms) error ϵ_{rms} is

$$\varepsilon_{rms} = \sqrt{\varepsilon_r^2 + \varepsilon_b^2} \quad (1.3)$$

The three selected frequencies correspond to the low frequency (highly colored), intermediate frequency (pink) and high frequency (almost white) behaviors. The distributions give additional information on the statistics of the estimates and are therefore of interest. The Gaussian distribution is plotted for reference and is entirely determined by the sample mean and variance of the spectral estimates at a selected frequency bin. The chi-square distribution is characterized by the mean of the estimates and the number of degrees of freedom. The analytical expression for the chi-square with mean μ and order n is given by [5]

$$P(x) = \left[2^{\frac{n}{2}} \Gamma\left(\frac{n}{2}\right) \right]^{-1} \left[\frac{n x}{\mu} \right]^{\frac{n}{2}-1} e^{-\frac{x n}{2\mu}} \quad (1.4)$$

where Γ is the Gamma function.

Otherwise stated, the selection of the fitted chi-square distribution is based, in each case, on the chi-square goodness of fit test [5] using 10 constant intervals. The discrepancy between the sample histogram and the fitted chi-square is measured by

$$\chi^2 = \sum_{i=1}^{10} \frac{(f_i - F_i)^2}{F_i} \quad (1.5)$$

where f_i is the observed number of observations and F_i the number of observations corresponding to the fitted distribution in the i^{th} interval.

The acceptance region of the fit between the sample histogram and the chi-square distribution at the $\alpha = 0.05$ level of significance is

$$\chi^2 \leq \chi^2_{8,0.05} \quad (1.6)$$

The number of degrees of freedom for which χ^2 is calculated is 8 since there are 9 independent frequencies f_i and the mean of the fitted distribution is estimated by the sample mean. The chi-square goodness of fit therefore produces a rough estimate of the number of degrees of freedom of the estimates which is a simple characterization of the distribution, assuming it follows a chi-square law.

3. Outline Of The Multiple Window Method

The multiple window (MW) method is described at length in [1,2,3]. It is not the purpose of this section to give a complete mathematical derivation of the method which starts with the Cramer spectral representation of random processes. Rather the goal of this paragraph is to give, in a short summary, background information on the MW method.

The MW method is a non parametric spectral estimation method based on multiple windowed Fast Fourier Transforms. The computation of the multiple windows, also called the Slepian windows, is a preliminary step. The method uses a subset S of orthonormal windows that are the eigenfunctions of

$$\gamma(f) = \int \frac{\sin \pi N(f-v)}{\sin \pi(f-v)} dZ(v) \quad (2.1)$$

where the bounds of the integral can be either $-\frac{1}{2}, \frac{1}{2}$ or $-W, W$ (W is the half

bandwidth of the window, a frequency parameter that characterizes the MW estimates, given N data points), $y(f)$ is the Discrete Fourier Transform of the data sequence of length N , $dZ(v)$ is the unknown, related to the power spectral density $S(f)$ by

$$E[|dZ(f)|^2] = S(f) df \quad (2.2)$$

The driving idea lies in the expansion of the solution $dZ(v)$ in term of the eigenfunctions. The subset S includes the $2NW$ windows that have the most concentrated energy in the bandwidth $2W$ (it is understood that $2NW$ is the integer part of $2NW$), the energy content of a window corresponds to its eigenvalue, λ_k , associated to the integral equation (2.1). Bias, which can be thought of as noise, increases as one keeps higher and higher order windows with lower and lower energy and can be evaluated by its upper bound given by the Schwartz inequality

$$\hat{B}_k(f) \approx \sigma^2(1 - \lambda_k) \quad (2.3)$$

where σ^2 is the power of the data sequence.

The $2NW$ Discrete Fourier Transforms of the data, windowed by each one of the $2NW$ windows, are then computed; the inferred spectra, $\hat{S}_k(f)$, are called eigenspectra. The Slepian windows give limited statistical consistency to the eigenspectra; windowing is interpreted in the frequency domain as an averaging over the bandwidth of the window, that is $2W$.

To get better variance control, the eigenspectra are finally averaged using adaptive weights that minimize the mean squared error of the spectral estimate. The final estimate $\hat{S}(f)$ is solution of

$$\sum_{k=0}^{2NW-1} \frac{\lambda_k \left[\hat{S}(f) - \frac{\lambda_k}{2NW} \left[\sum_{k=0}^{2NW-1} \lambda_k^{-1} \right] \hat{S}_k(f) \right]}{\left[\lambda_k \hat{S}(f) + \hat{B}_k(f) \right]^2} = 0 \quad (2.4)$$

Because of the orthonormality of the windows, degrees of freedom are indeed added, thus producing a consistent estimator.

The method is easily extended to mixed spectra using statistical tests (Fisher's statistic test) to detect line components in the spectrum. The spectrum is corrected or reshaped once a line component is detected. The power in the line component is subtracted from the spectrum over a $2W$ wide frequency zone around the sinusoid by using a local expansion of the spectrum on the Slepian windows.

The estimates of the power spectrum discussed hereafter corresponds to (2.4) which is implemented in the Fortran programs written by Allan D. Chave. These programs are such that they yield correct power for white noise [2]. This paper only deals with continuous spectra, although one of the strength of the MW method is its ability to handle mixed spectra.

As pointed out in [1,2,3] a good compromise between variance, bias and resolution is achieved for a time bandwidth product NW of 4. The MW method has the reputation of working well on short data sequence, offering good variance control, good bias protection and fair resolution. To quantify the MW characteristics, the selected data length for the numerical simulations is $N=128$.

4. Outline Of The Maximum Likelihood Method

As mentioned in §3, the Multiple Window method combines with classical Fast Fourier Transforms a data adaptive technique to weight the eigenspectra and produce the final spectral estimate. It is thus of interest to compare the MW results with those of a classic data adaptive estimation method such as the Maximum Likelihood method also called the Minimum Variance method [6,7,8].

The Maximum Likelihood (MLM) method designs an optimal finite impulse response filter that minimizes the output power or variance and passes the center frequency undistorted. The power spectrum is given by

$$\hat{S}(f) = \frac{p}{e^H R^{-1} e} \quad (3.1)$$

where R^{-1} is the inverse of the autocorrelation matrix of order p , H the Hermitian operator and e is the complex sinusoid vector

$$e(f) = \left[1 \quad e^{j2\pi f T} \quad \dots \quad e^{j2\pi f T p} \right]^t \quad (3.2)$$

t represents the transpose operation, f the frequency and T the sampling period.

Several computational methods can be used : a direct inversion of the autocorrelation matrix (considering the possibility of the matrix being singular as described in [6]), or an indirect determination of the power spectrum using a relationship between the Maximum Likelihood estimate and the AR spectral estimate [7,8]. The method used in this simulation computes an estimate of the autocorrelation matrix and inverts it. A check for singular matrix is performed. The singular matrices can be stabilized by adding a small number to the main diagonal.

The power spectrum is then computed by Fast Fourier Transforms, on the basis of equation (3.1) rewritten as

$$e^H R^{-1} e = (e^H (R^{-1})^t)^* e^* \quad (3.3)$$

where $*$ is the complex conjugate. The sequence of operations is

- (1) the inversion of the autocorrelation matrix R (a Toeplitz matrix)
- (2) the transposition of R^{-1}
- (3) the FFT of all the columns of the matrix R^{-1} giving a (N_{FFT}, p) matrix
- (4) the complex conjugation of the (N_{FFT}, p) matrix of step 3
- (5) the FFT on all the lines of the (N_{FFT}, p) matrix of step 4, giving a (N_{FFT}, N_{FFT}) matrix

The power spectrum is recovered by taking the inverse of the real part of each element of the main diagonal of the (N_{FFT}, N_{FFT}) matrix of step 5. It is then normalized by the sampling time, multiplied by 2 to yield the proper one-sided spectrum levels and finally multiplied by p , the order of the autocorrelation matrix R , to yield proper power for a white noise [8].

5. Ambient Noise Data

An ARMA process of order (1,n) is used to model the ambient noise and create the simulation data. Typical ambient noise, as given in [4], can be approximated in a straightforward manner by a transfer function of the form

$$H(z) = \frac{1 + \sum_{k=1}^l a_k z^{-k}}{1 + \sum_{k=1}^n b_k z^{-k}} \quad (4.1)$$

By visual selection of the poles and zeros of this transfer function on the z plane, a theoretical frequency response close in shape to an ambient noise spectrum can be created.

Using an iterative process, five poles were selected at

$$z = 0.99$$

$$z = 0.7886876 \pm i 0.452389$$

$$z = 0.899868 \pm i 0.015707$$

and four zeros at

$$z = 0.895456 \pm i 0.090326$$

$$z = 0.8966357 \pm i 0.080891$$

Poles and zeros are respectively plotted on Figure 5.1.

The corresponding ARMA process of order (4,5) has the following transfer function

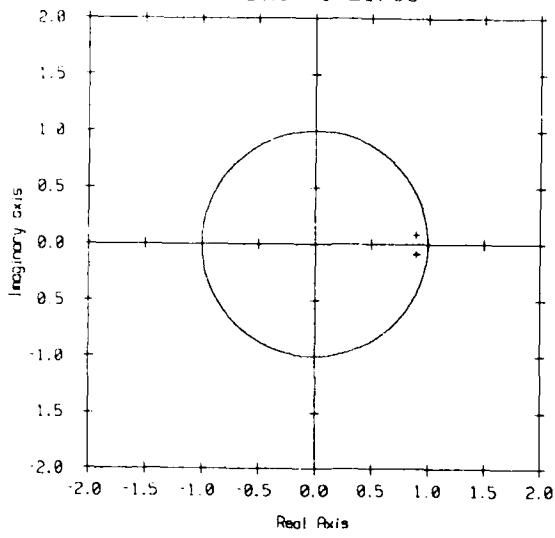
$$H(z) = \frac{1 - 3.5836 z^{-1} + 4.8306 z^{-2} - 2.90272 z^{-3} + 0.6561 z^{-4}}{1 - 4.3671 z^{-1} + 7.8188 z^{-2} - 7.1962 z^{-3} + 3.4074 z^{-4} - 0.66291 z^{-5}} \quad (4.2)$$

The corresponding frequency response is plotted on Figure 5.2.

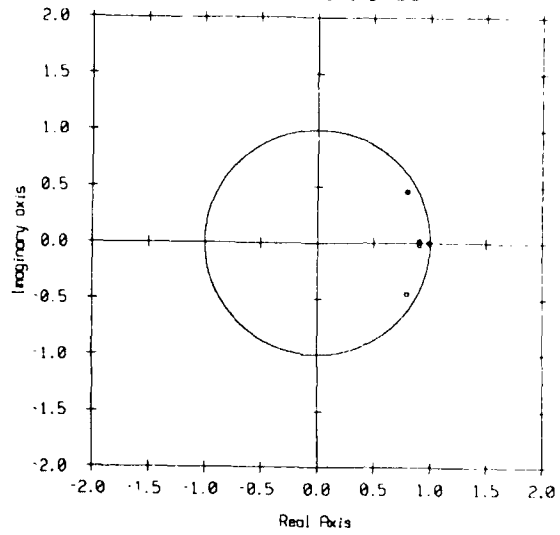
The driving sequence is a centered white Gaussian noise with unit variance. The ARMA process is readily implemented as finite impulse response and infinite impulse response filters.

1024 points of the data sequence are plotted on Figure 5.3. This data sample corresponds to 2.05 seconds with a sampling frequency of 500 Hz. The theoretical one sided "ambient noise" spectral density is plotted between DC and 250 Hz on Figure 5.4.

Zeros of Noise Filter
Transfer Function 3/21/88



Poles of Noise Filter
Transfer Function 3/21/88



Noise Filter Transfer Function
3/21/88

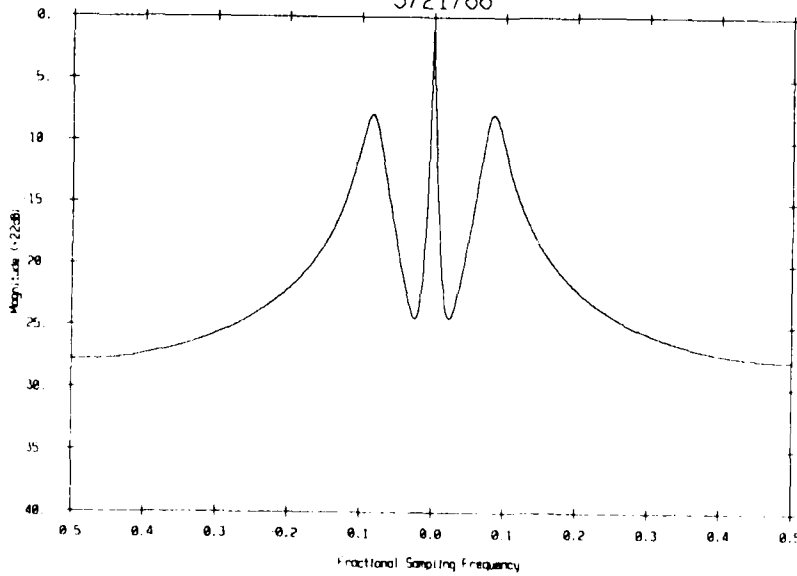


Figure 5.1 Zeros and poles of the ARMA process

Figure 5.2 Transfer function of data generating filter

Simulated Ambient Noise
Using an ARMA process (2.05 s of data)

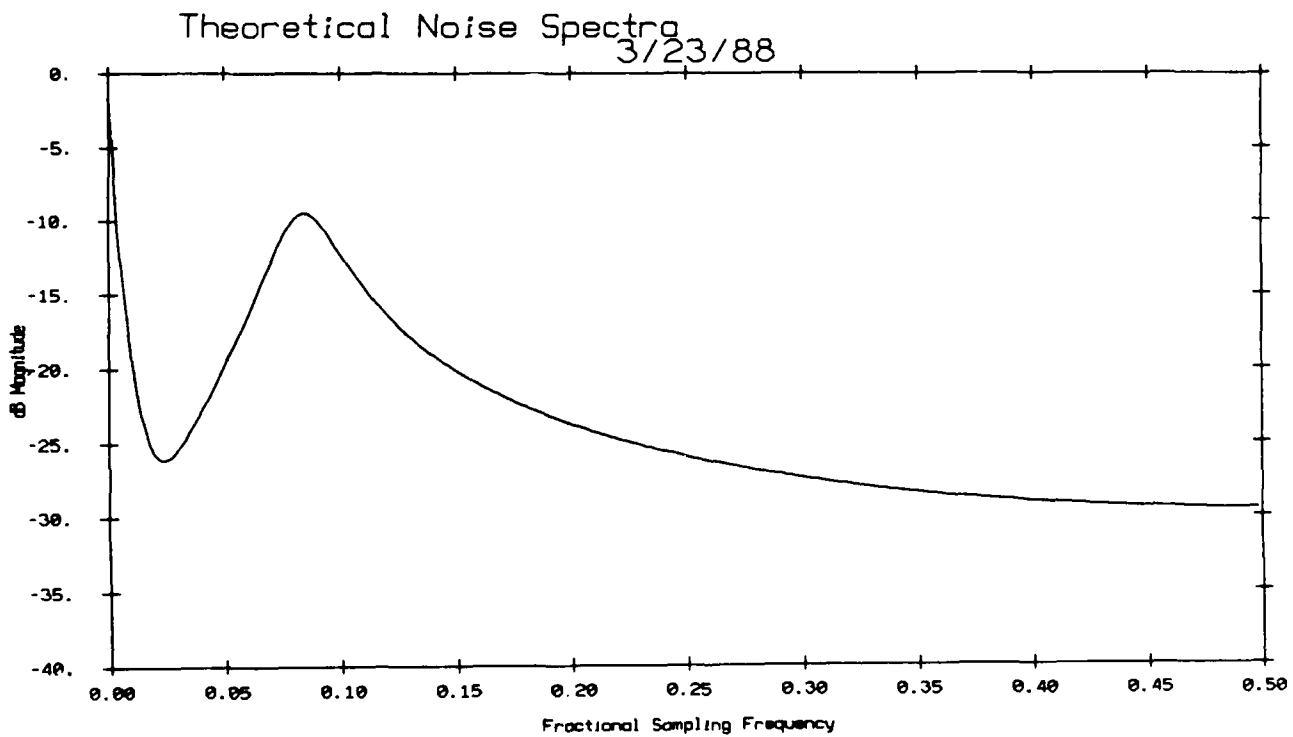
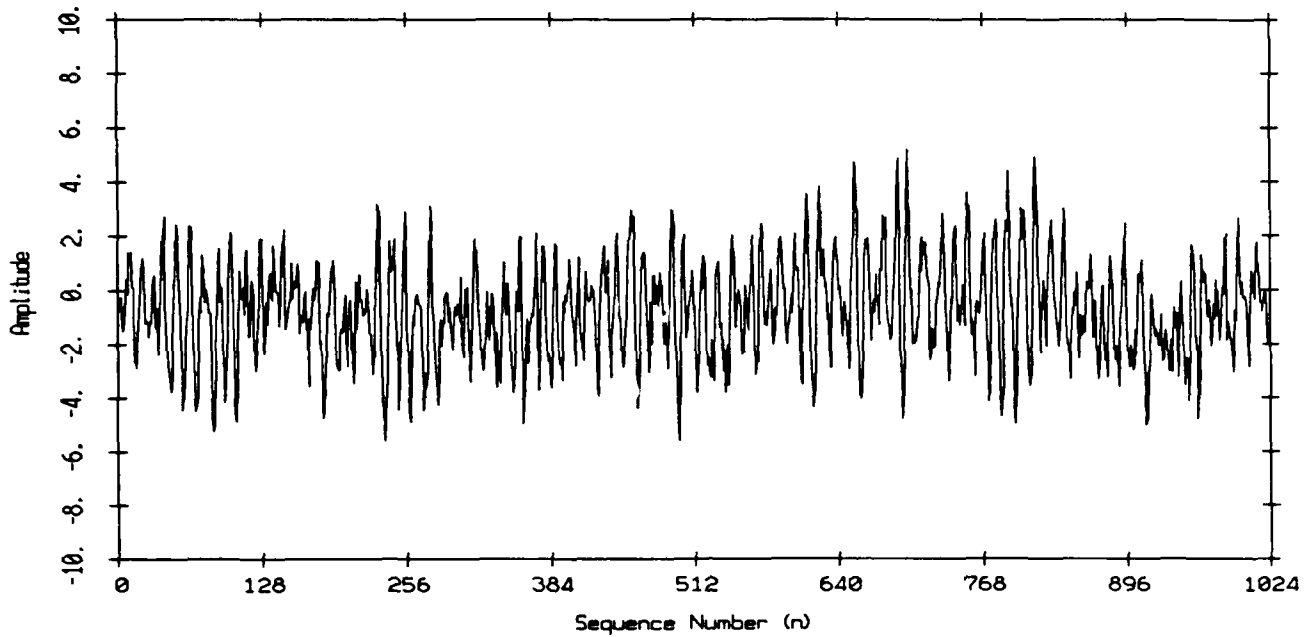


Figure 5.3 Simulated noise data sequence (1024 points)

Figure 5.4 Theoretical "ambient" noise power spectral density

6. Averaged Periodogram Estimate

The reference periodogram estimates are incoherent averages of eight FFTs with a Hanning window, the transforms are performed on 128 data points with an overlap of 50 %. The length of the FFT is 512 (i.e. 128 data points zero-padded out to the FFT length of 512). Each periodogram estimate thus is based on 576 data points.

A fairly small data length is used in the transform because of the MW method capability to work on short data sequences. The number of averaged FFTs corresponds to the numerical workload of the MW method when the time bandwidth product NW is 4 and the number of windows $2NW$ is 8.

512 different spectra were computed on the simulated ambient noise time series and are overlaid on Figure 6.1. The envelope and the mean of these 512 estimates are plotted on Figure 6.2. The mean gives an idea of the estimate bias with respect to the theoretical ambient noise spectrum (Figure 5.4). The envelope gives an idea of the scatter or variance of the FFT based estimates. The ambient noise spectrum is well resolved by this classic method.

The random error ϵ_r is plotted on Figure 6.3 and varies between 0.35 and 0.40. The spectral estimate is the average of n_d raw spectra. It approximately follows a chi-square distribution with $2n_d$ degrees of freedom. The random error is evaluated by the ratio of the standard deviation of the estimate to its mean [5] giving $1/\sqrt{n_d}$; in the present case the random error should theoretically be 0.35.

The bias error ϵ_b plotted on Figure 6.4 is low, below 0.2, except at low frequencies where it peaks up to 2.75. The rms error ϵ_{rms} is dominated by the random error. It is plotted on Figure 2.5 and is bounded by 0.35 and 0.4 except at low frequency where it goes up to 3.46.

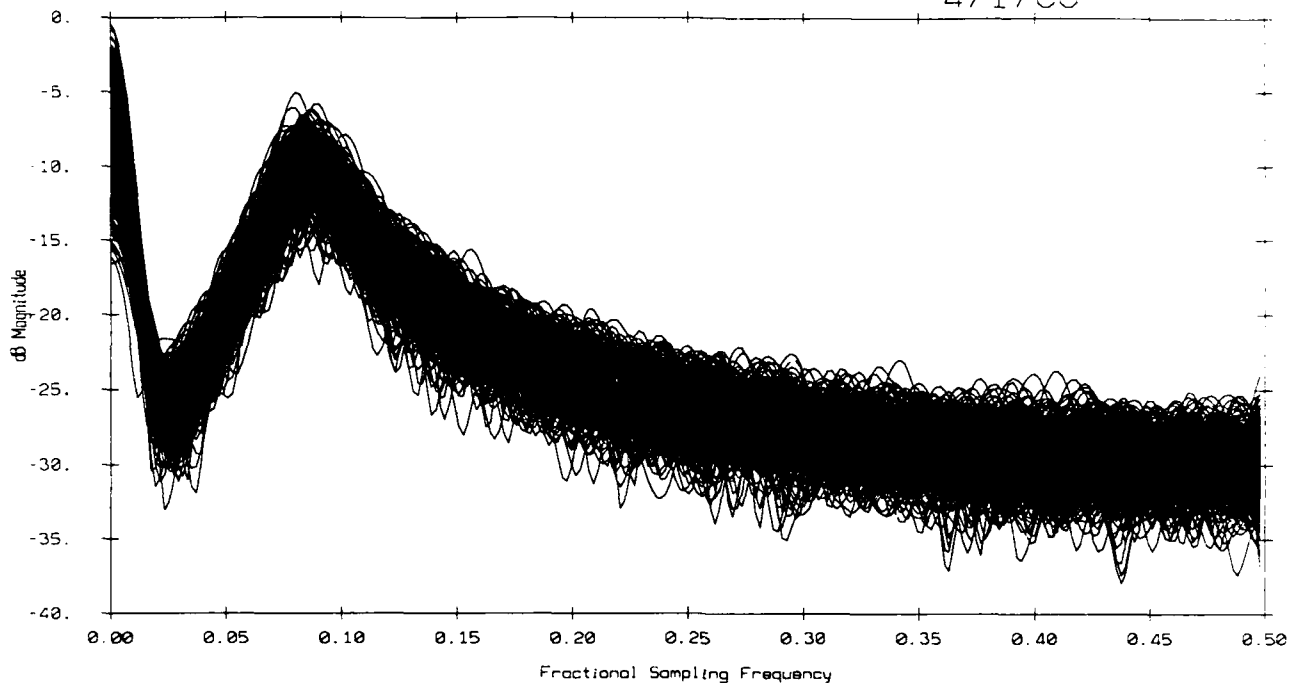
As mentioned before, the distribution of the estimates is theoretically a chi-square distribution with 16 degrees of freedom. Fitted Gaussian and fitted chi-square distributions are compared to the histograms of the spectral estimates at the selected frequencies (§2). They are respectively plotted on Figures 6.6, 6.7 and 6.8. There is indeed good agreement in term of the number of degrees of freedom of the estimate since they are respectively 16, 16 and 14 at the normalized frequencies 10/512, 50/512 and 200/512.

Normalized Errors			
	ϵ_r	ϵ_b	ϵ_{rms}
Characteristic value	0.4	< 0.2	0.4
Maximum Value	2.1	2.75	3.46

Approximate Number of Degrees of Freedom			
Normalized Frequency	10/512	50/512	200/512
Degrees of Freedom	16	16	14

512 FFT based Spectra

4/1/88



Mean and Envelope of 512 FFT based Spectra

4/1/88

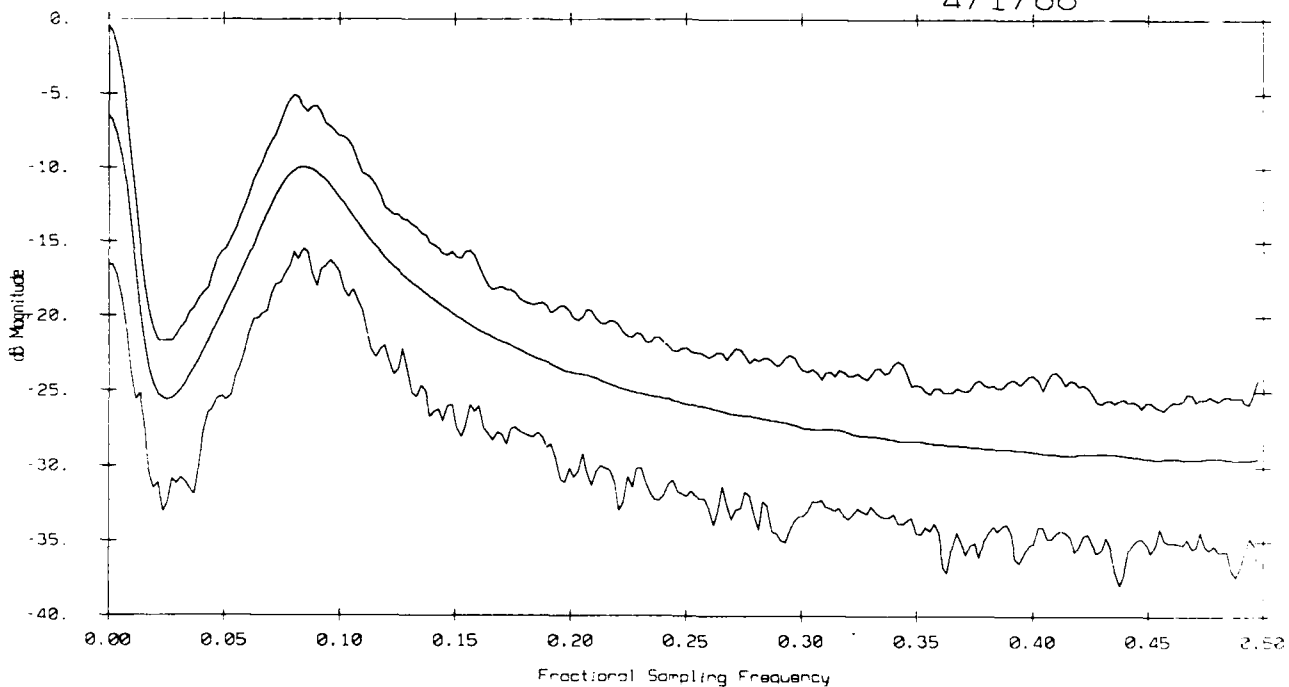


Figure 6.1 512 overlaid conventional FFT spectral densities (8 incoherent averaged FFTs on 128 points with a Hanning window)

Figure 6.2 Mean and envelope of the 512 spectral density realizations

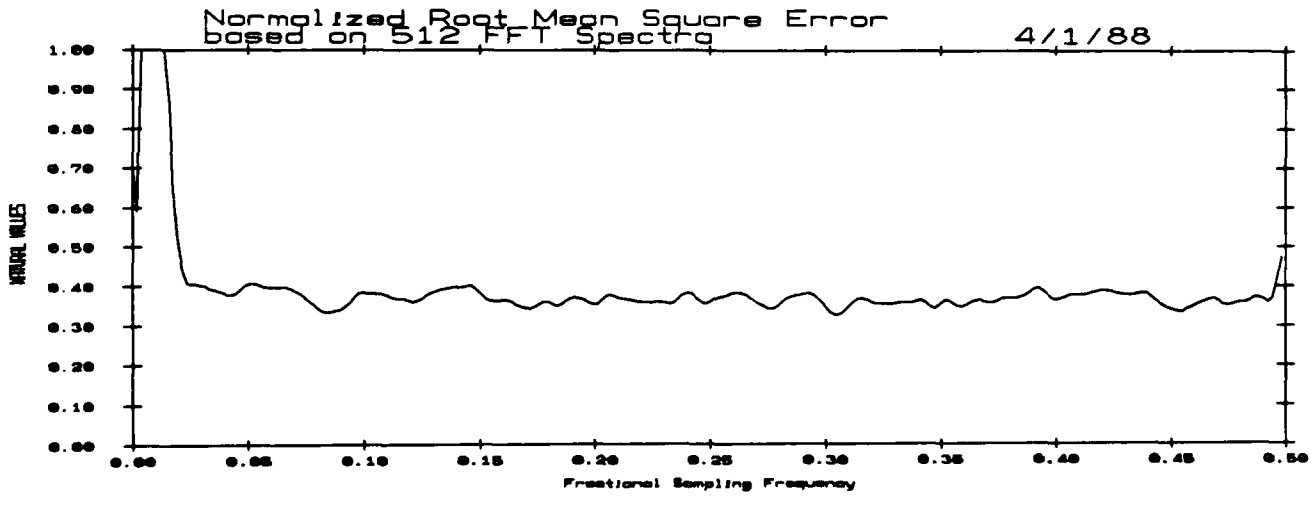
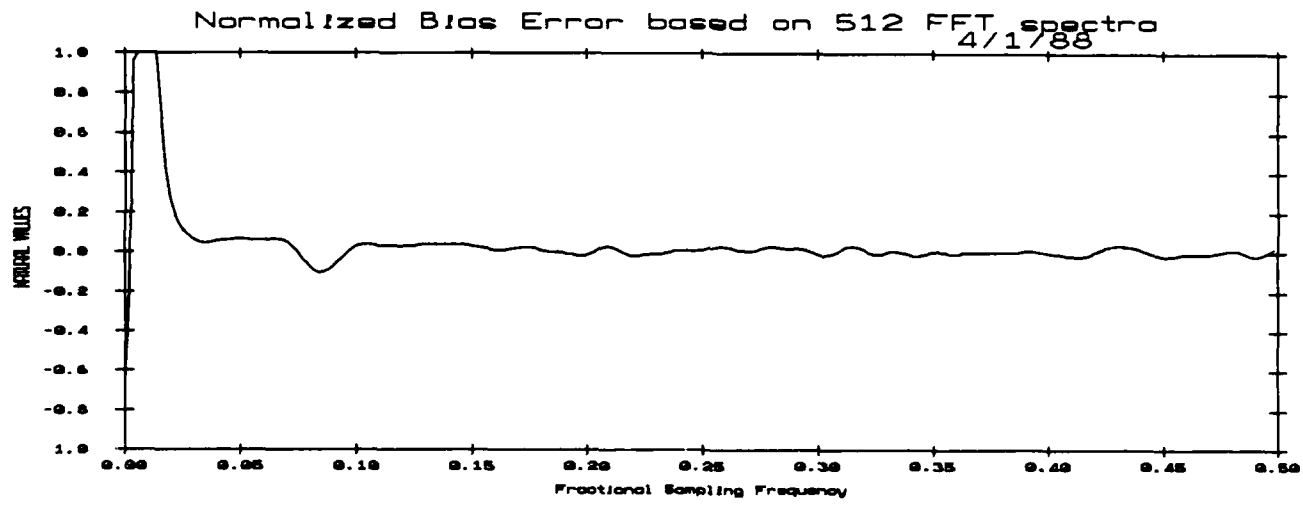
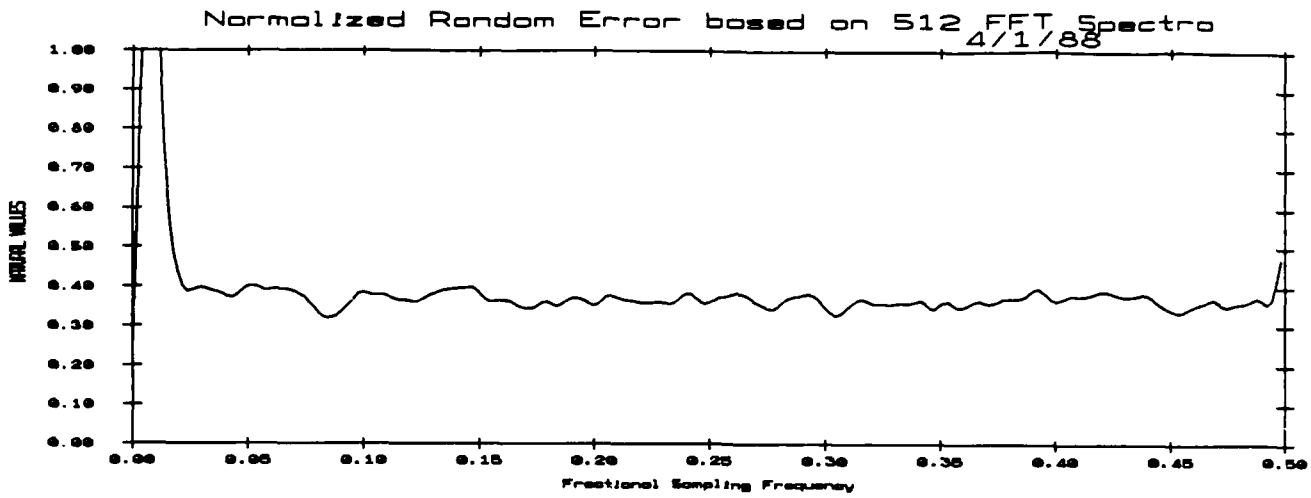


Figure 6.3 Normalized random error ϵ_r

Figure 6.4 Normalized bias error ϵ_b

Figure 6.5 Normalized rms error ϵ_{rms}

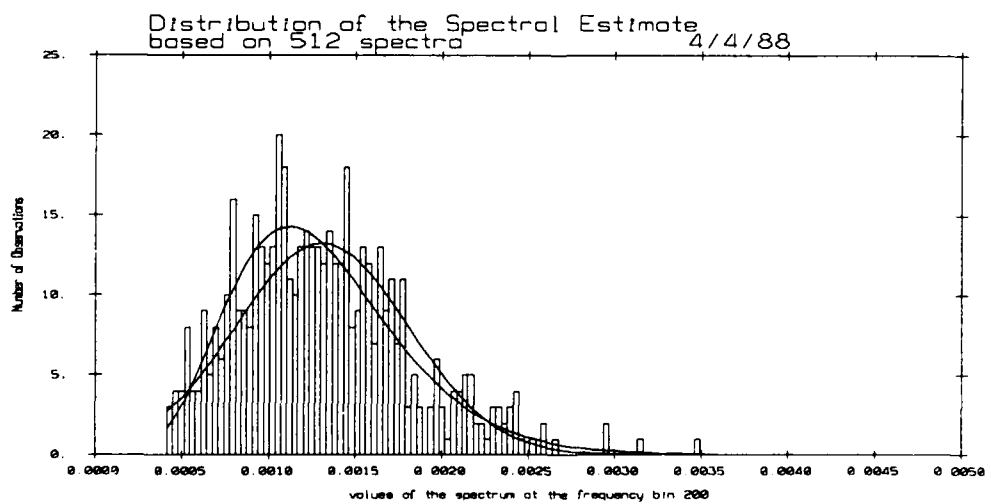
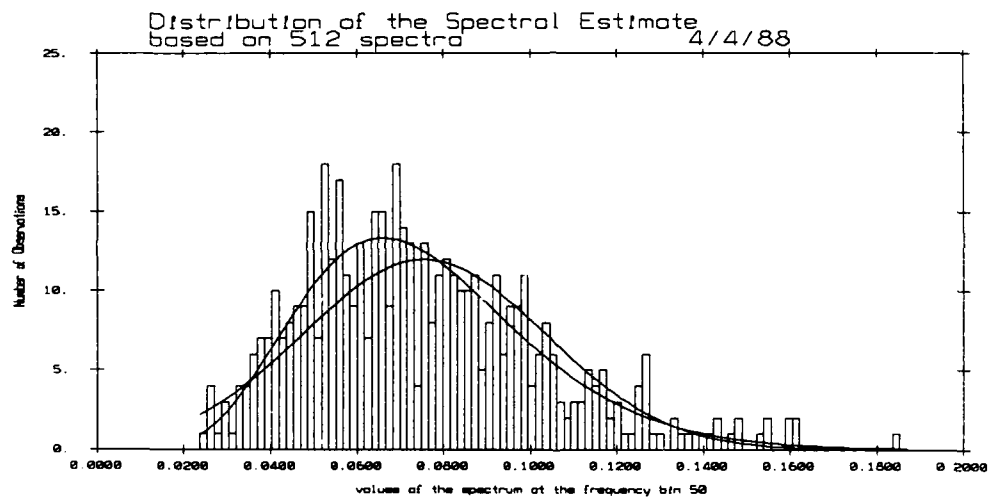
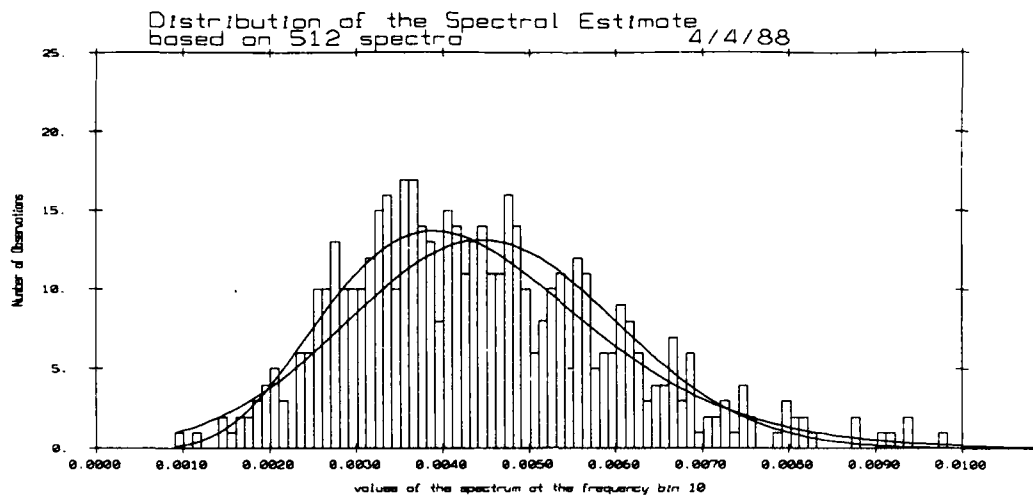


Figure 6.6 Sample histogram at the normalized frequency 10/512 overlaid with fitted Gaussian and χ^2_{16} distributions

Figure 6.7 Sample histogram at the normalized frequency 50/512 overlaid with fitted Gaussian and χ^2_{16} distributions

Figure 6.8 Sample histogram at the normalized frequency 200/512 overlaid with fitted Gaussian and χ^2_{14} distributions

7. Multiple Window Estimate

7.1. Selection Of The Time Bandwidth Product NW

As stated earlier, the optimal time bandwidth product NW is 4. If the estimate is based on 128 points, the equivalent MW filter normalized bandwidth $2W$ is 0.0625. The main features of the simulated noise is a -25 dB dip at the normalized frequency 0.02 (or 8 Hz) which is followed, 15 dB higher, by a moderate Q resonance (shipping bump) just before the normalized frequency 0.01 (or around 50 Hz). One can already predict that these features will be smeared by the equivalent filtering of the multiple windows, thus leading to a significant bias of the estimate at low frequency, if such a time bandwidth product is selected.

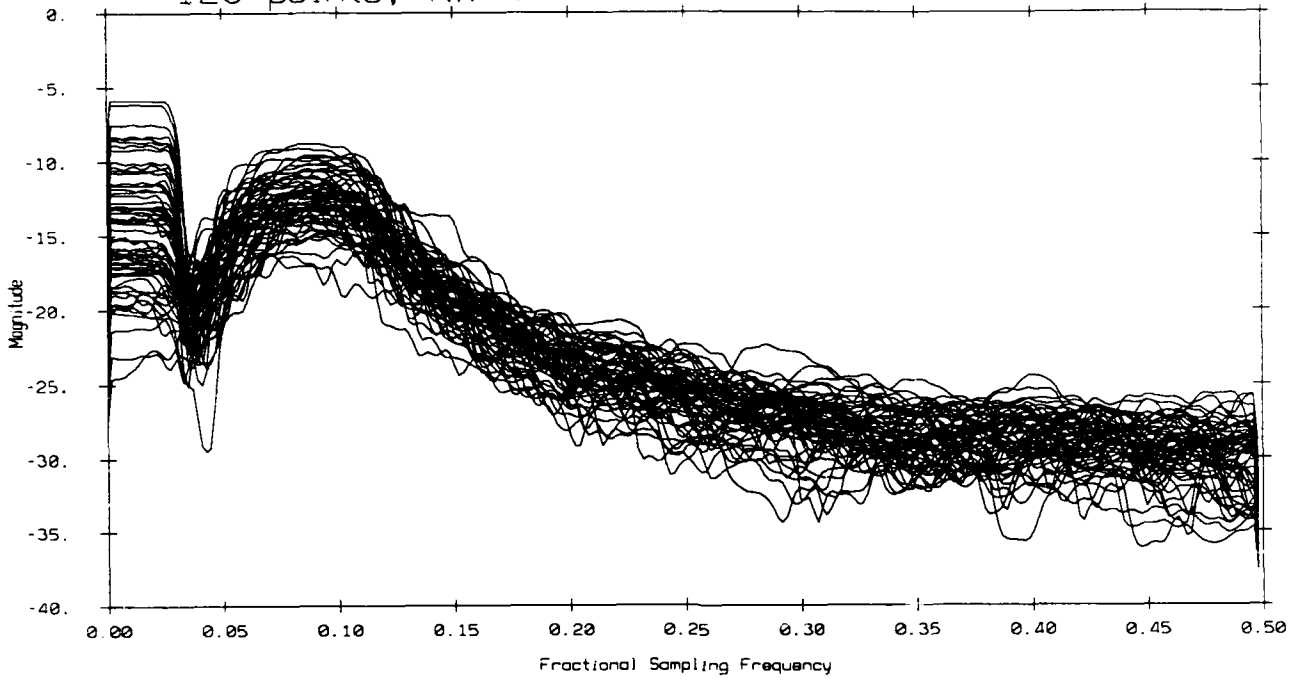
To illustrate this point, 64 spectra were computed on the first 128 points of each periodogram 576 point long sequence. NW is 4 and the number of windows is 8. No reshaping was performed since there is no line component in the data. The smearing effect is clearly seen on Figure 7.1.1 and Figure 7.1.2 where the overlaid spectra and the mean and envelope of the 64 estimates are plotted.

The very red spectral zones are smeared near DC where the spectrum is flat up to a frequency that corresponds to the half averaging filter bandwidth W . The resonance is broader, with a lower Q than the theoretical one.

When the time bandwidth product is 4, the averaging equivalent filter bandwidth is too large to be able to resolve the structure of the simulated ambient noise. In order to see more details in the spectrum estimate, one has to decrease the time bandwidth product but the drawback is more variance in the estimate [1,2,3].

The analysis, described in §2 and carried out in §5, is repeated for two time bandwidth products $NW = 2$ and $NW = 3$. Then, to compare the classical FFT based method and the MW method on the basis of the same information, MW estimates are computed on the same 576 point sequences as in §6, with a time bandwidth product NW of 4 and 8 windows.

64 Overlaid Window Based Power Spectra
128 points, NW=4



Mean and Envelope of 64 MW Spectra
128 points, NW=4, kspec=8 3/23/88

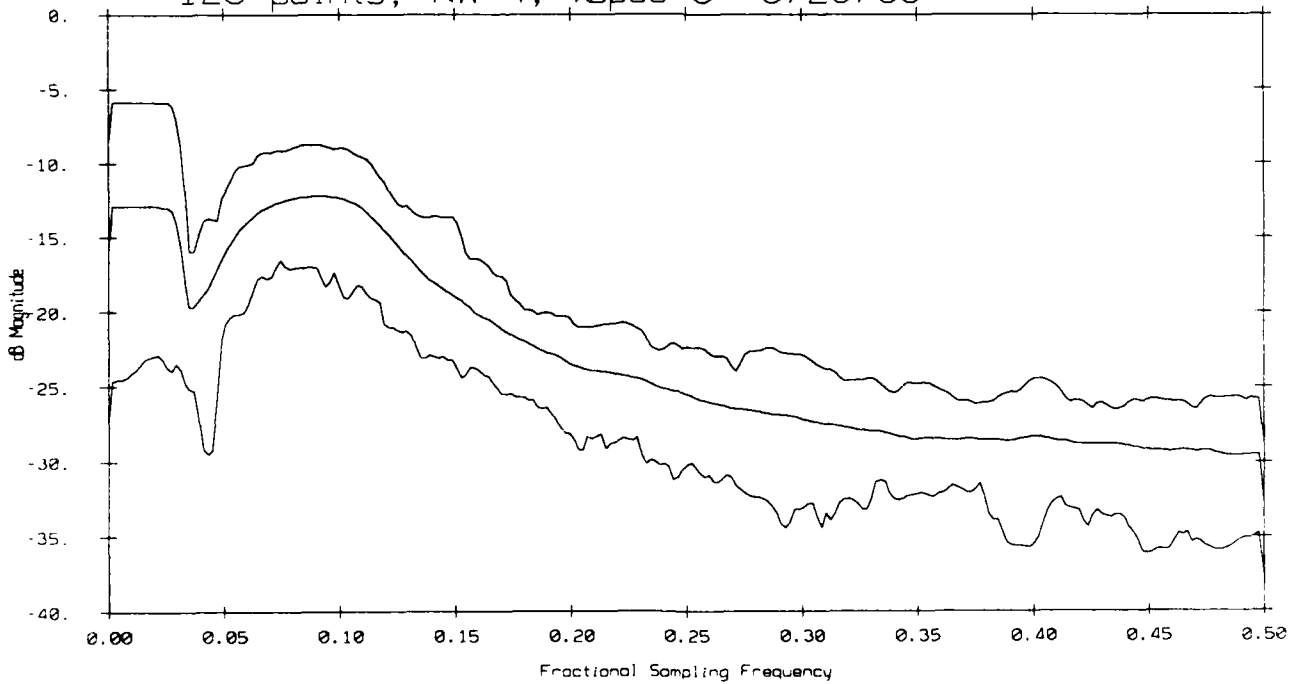


Figure 7.1.1 64 overlaid spectral densities computed by the MW method on 128 points with a time bandwidth product NW of 4

Figure 7.1.2 Mean and envelope of the 64 spectral densities

7.2. MW Estimate On 128 points With $NW = 2$

512 spectra were computed based on the first 128 points of the FFTs 576 point long sequence. The time bandwidth product NW is 2, the number of windows 4 and no reshaping is performed. The Fourier transforms are done on 512 points. The 512 MW spectra are overlaid on Figure 7.2.1 and the mean and envelope of the 512 estimates are plotted of Figure 7.2.2.

Because the averaging MW filter normalized bandwidth is only 0.03125, the noise dip around the normalized frequency 0.0625 (or 8 Hz) is resolved and the overall shape of the mean spectrum fits the theoretical one. Nevertheless, there is some smearing effect at DC due to the MW averaging filter and there is much more scatter than for the FFT estimates.

The random error ϵ_r is plotted on Figure 7.2.3. It is higher than for the periodogram estimates since it varies around 0.6 at high frequency, the random error has a maximum of 16.9. The bias error ϵ_b is plotted on Figure 7.2.4 and it is also slightly higher than the FFT one, although bounded by 0.2 at high frequencies with a maximum at low frequency equal to 13.26. The rms error ϵ_{rms} is therefore higher than the periodogram rms error and oscillates around 0.6 at high frequencies as shown on Figure 7.2.5. The rms error maximum is 21.52 at low frequency.

Distributions and histograms at the pre-selected frequencies (§2) are plotted on Figures 7.2.6, 7.2.7, 7.2.8. Since the number of windows $2NW$ is 4, one can expect a number of degrees of freedom smaller or equal to 8. The distribution at low frequency (10/512) does not follow a chi-square distribution of any order. The χ^2 surimposed on the histogram is rejected by the chi-square goodness of fit test at the $\alpha = 0.05$ level of significance. The MW method at low frequency has a poor distribution. One can estimate the number of degrees of freedom to be smaller than 2, which means that, as a result of the adaptive weighting, only one eigenspectrum is used in the MW estimate.

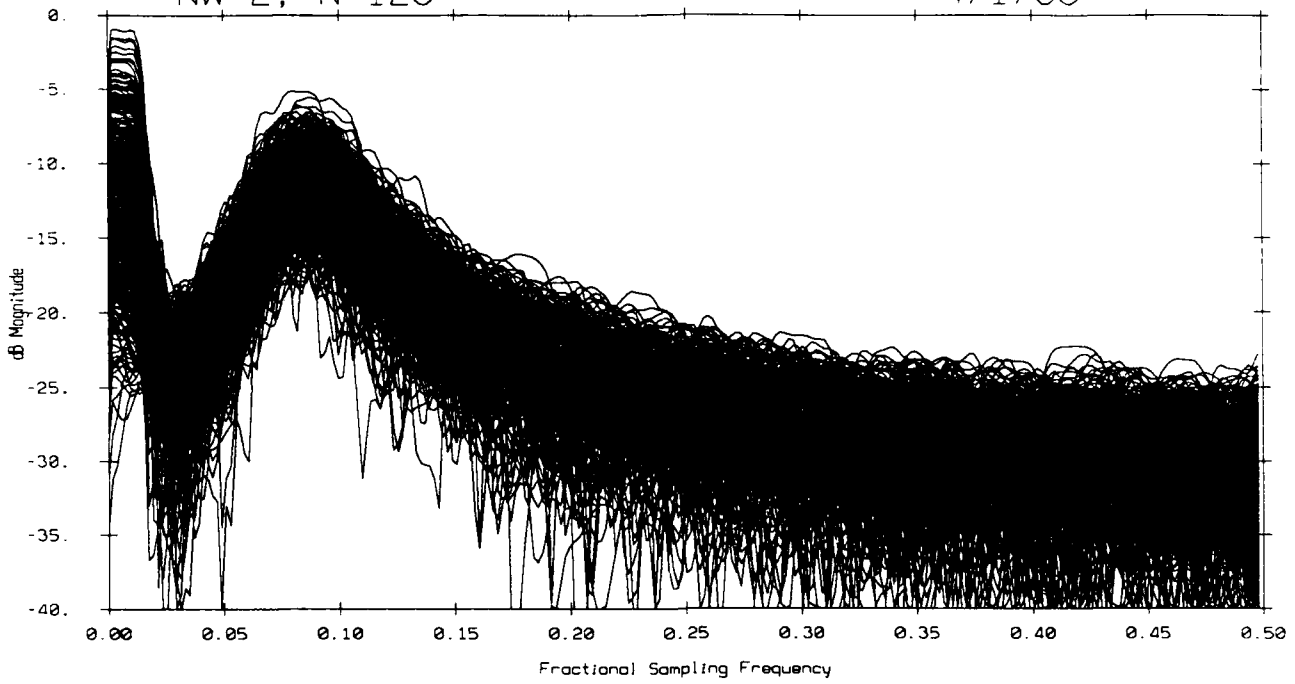
The distribution at intermediate frequency (50/512) follows a chi-square distribution with 8 degrees of freedom while at higher frequency (200/512) the number of degrees of freedom is only 6.

Table 7.2.1			
Normalized Errors			
	ϵ_r	ϵ_b	ϵ_{rms}
Characteristic Value	0.6	0.2	0.6
Maximum Value	16.9	13.26	21.52

Table 7.2.2			
Approximate Number of Degrees of Freedom			
Normalized Frequency	10/512	50/512	200/512
Degrees of Freedom	< 2	8	6

512 MW based Spectra
NW=2, N=128

4/1/88



Mean and Envelope of 512 MW based Spectra
4/5/88

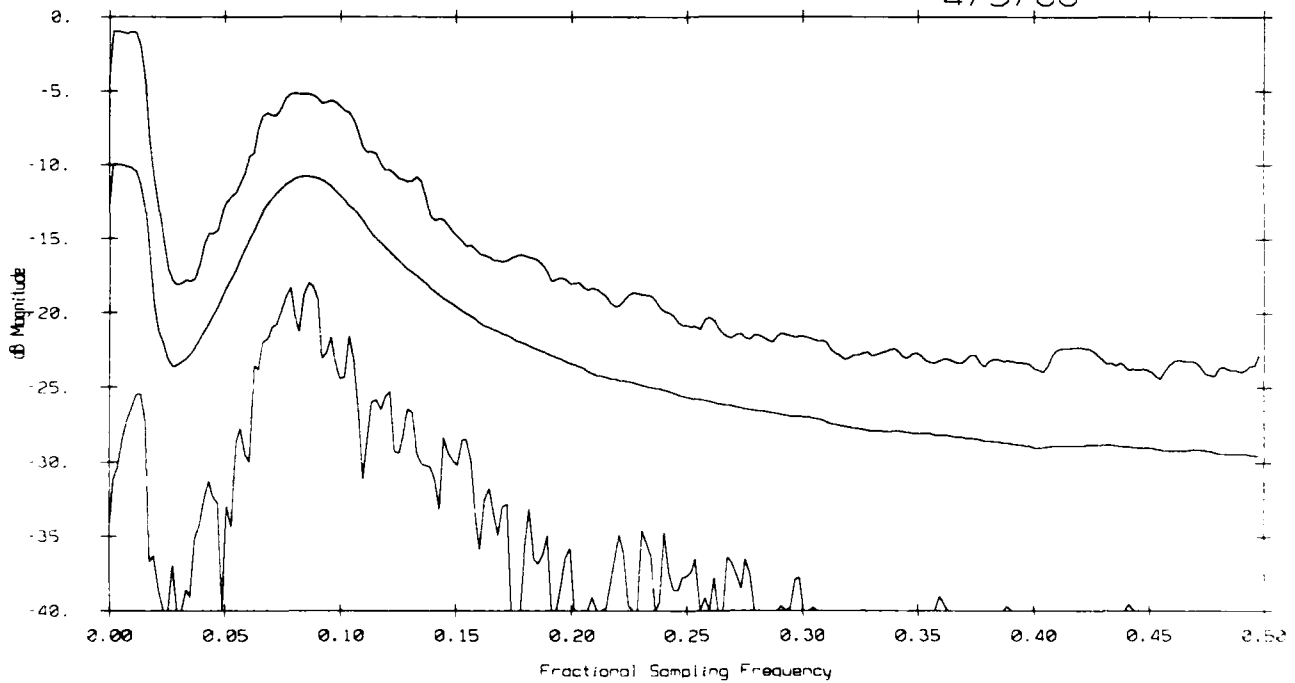


Figure 7.2.1 512 overlaid spectral densities computed by the MW method on 128 points and a time bandwidth product NW of 2

Figure 7.2.2 Mean and envelope of the 512 spectral densities

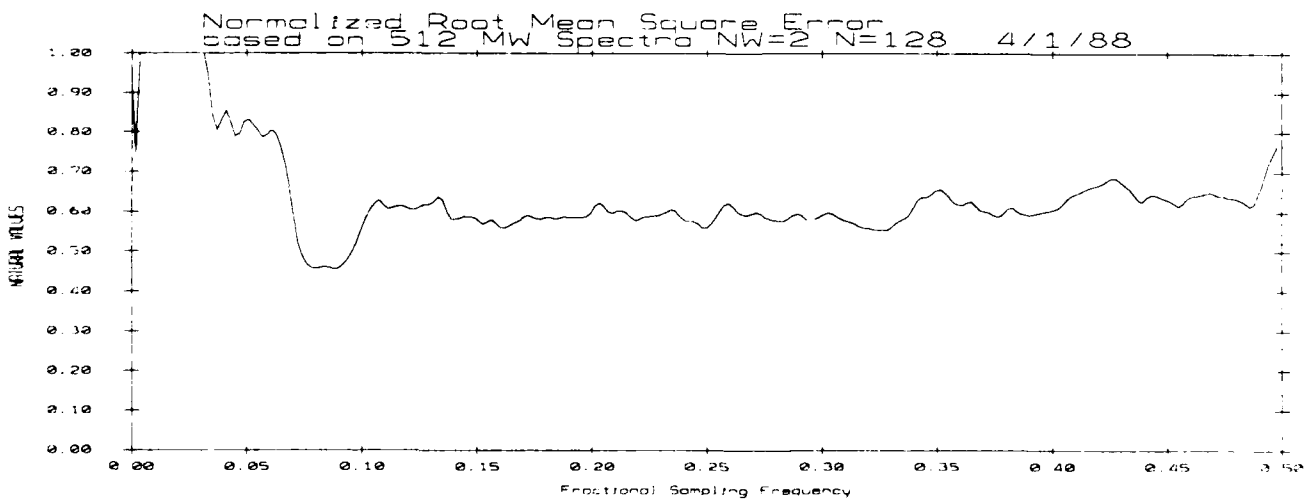
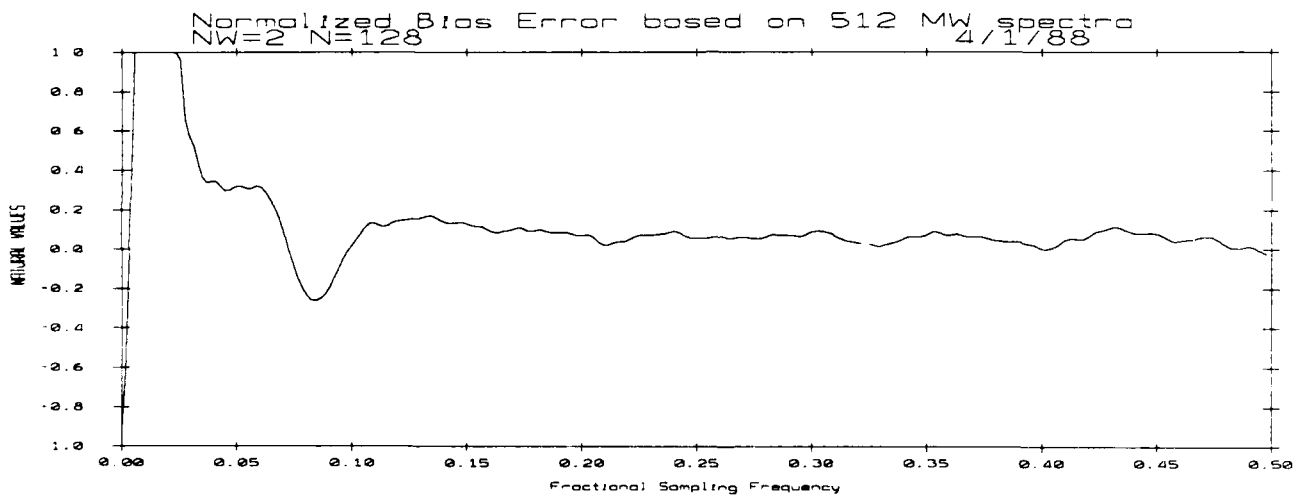
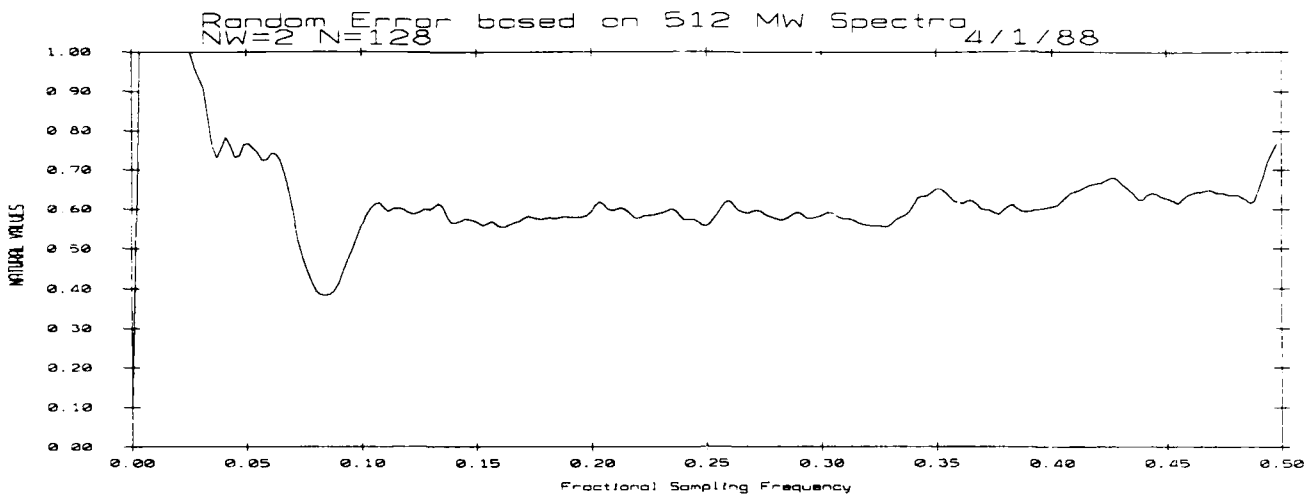


Figure 7.2.3 Normalized random error ϵ_r

Figure 7.2.4 Normalized bias error ϵ_b

Figure 7.2.5 Normalized rms error ϵ_{rms}

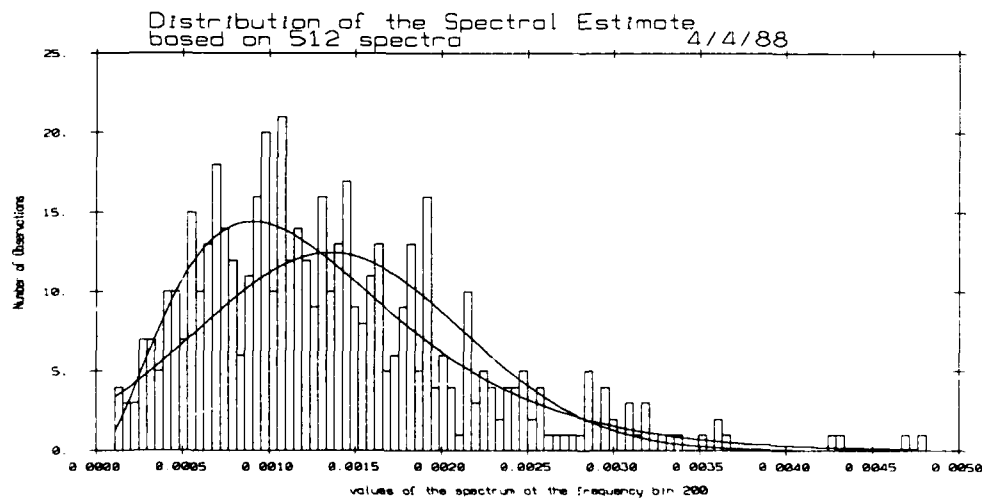
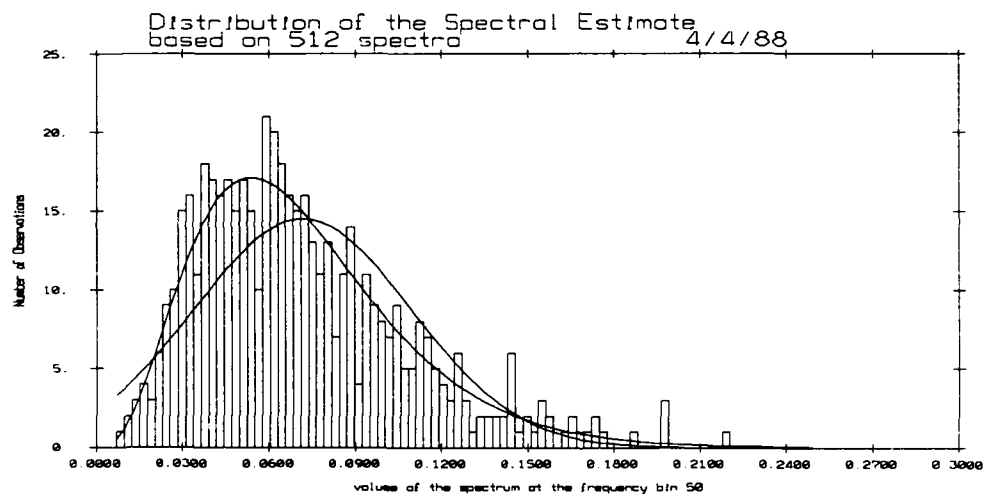
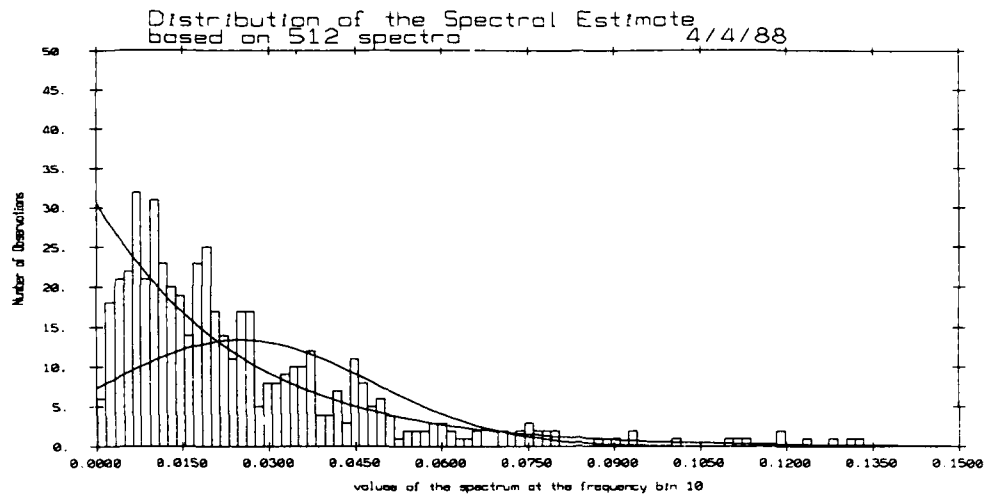


Figure 7.2.6 Sample histogram at the normalized frequency 10/512 overlaid with fitted Gaussian and χ^2_2 distributions

Figure 7.2.7 Sample histogram at the normalized frequency 50/512 overlaid with fitted Gaussian and χ^2_8 distributions

Figure 7.2.8 Sample histogram at the normalized frequency 200/512 overlaid with fitted Gaussian and χ^2_6 distributions

7.3. MW Estimate On 128 points With $NW = 3$

512 spectral densities were computed, as in §7.2 and on the same data, with a time bandwidth product NW of 3 and six windows. No reshaping was performed.

The overlaid spectra are plotted on Figure 7.3.1. The mean and envelope of the estimates are plotted on Figure 7.3.2. Since the averaging filter normalized bandwidth is 0.04687, the estimates are expected to have more bias but less variance [2,3]. There is indeed more smearing at DC than before and the shipping bump or power spectrum local maximum is slightly broader. On the other hand, one can easily visualize the decrease in variance with respect to the results of §7.2, where NW equal 2.

The random error ϵ_r , plotted on Figure 7.3.3, is essentially varying around 0.5, thus lower than for a time bandwidth product NW of 2. It has a maximum value of 26. The bias error ϵ_b , plotted on Figure 7.3.4, is at low frequency higher than for a time bandwidth product NW of 2, but at high frequency it is similar to the results of §6 (FFT estimates). The maximum value of ϵ_b at low frequency is 21.2. The rms error, plotted on Figure 7.3.5, is lower than for a time bandwidth product of 2 at high frequencies : 0.5 instead of 0.6. At low frequencies, where the spectrum is red, ϵ_r goes up to 33.55.

The distributions of the spectral estimates at the selected frequencies (§2) are plotted on Figure 7.3.6, 7.3.7 and 7.3.8. The number of degrees of freedom is expected to be smaller or equal to 12 since the MW estimate is an average of six eigenspectra. Like in §7.2, the low frequency (10/512) histogram does not follow a chi-square law of any order. The χ^2_2 surimposed on the histogram (Figure 7.3.6) was rejected by the chi-square goodness of fit at the $\alpha = 0.05$ level of significance. Once again, the distribution is poor and the corresponding number of degrees of freedom of estimate is smaller than 2.

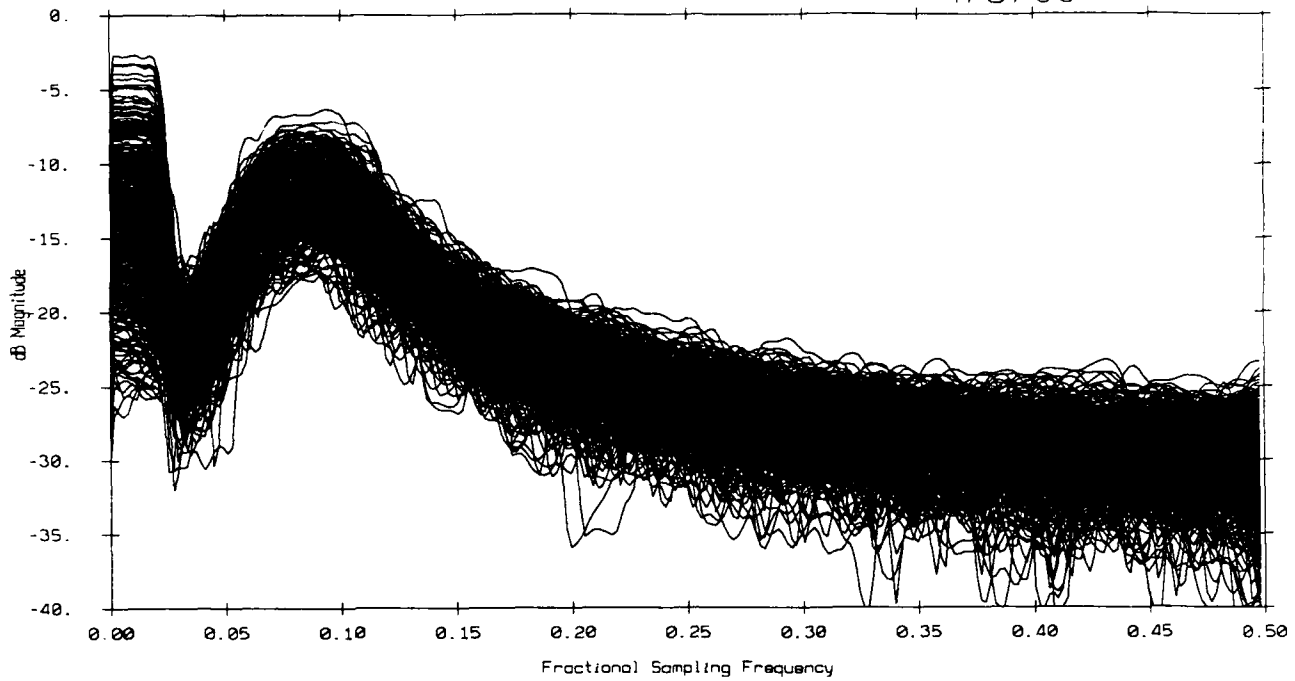
At intermediate and high frequency (50/512 and 200/512), the sample distribution is fitted by a χ^2_{10} .

Table 7.3.1			
Normalized Errors			
	ϵ_r	ϵ_b	ϵ_{rms}
Characteristic Value	0.5	< 0.2	0.5
Maximum Value	26	21.2	33.55

Table 7.3.2			
Approximate Number of Degrees of Freedom			
Normalized Frequency	10/512	50/512	200/512
Degrees of Freedom	< 2	10	10

512 MW Spectra NW=3 N=128

4/5/88



Mean and Envelope of 512 MW based Spectra
NW=3 N=128

4/5/88

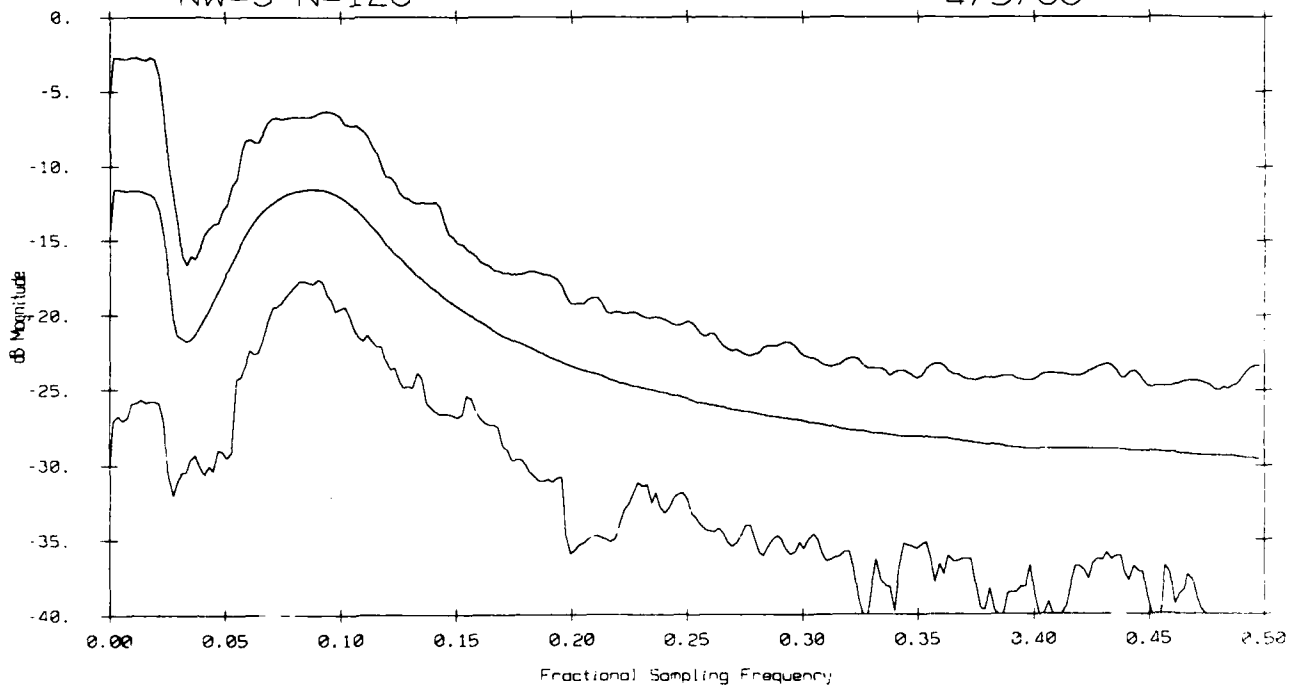


Figure 7.3.1 512 overlaid spectral densities computed by the MW method on 128 points with a time bandwidth product NW of 3

Figure 7.3.2 Mean and envelope of the 512 spectral densities

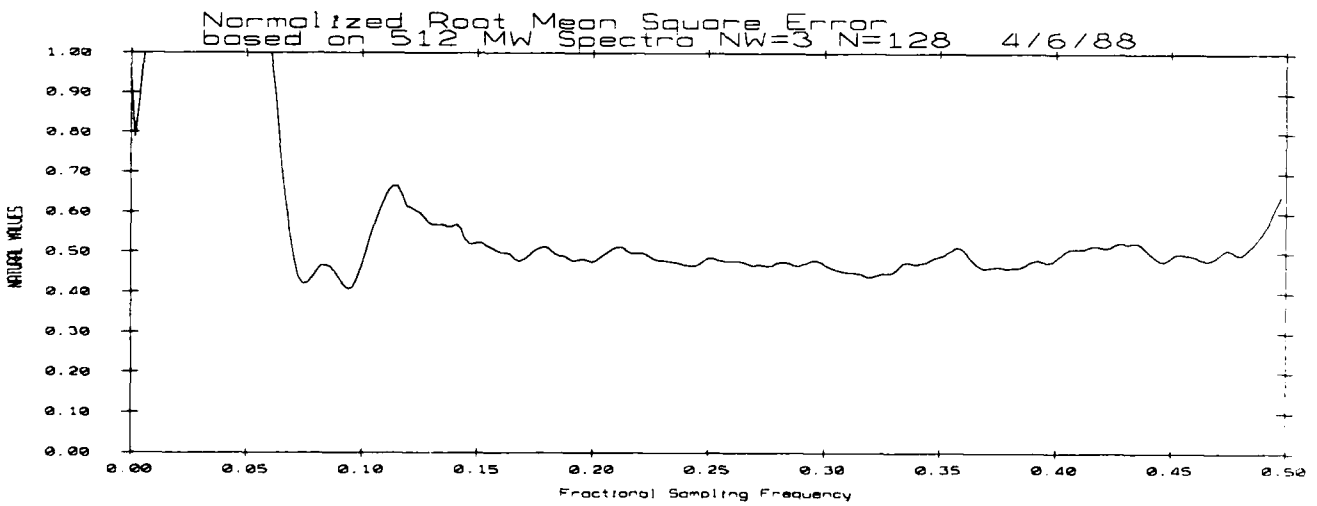
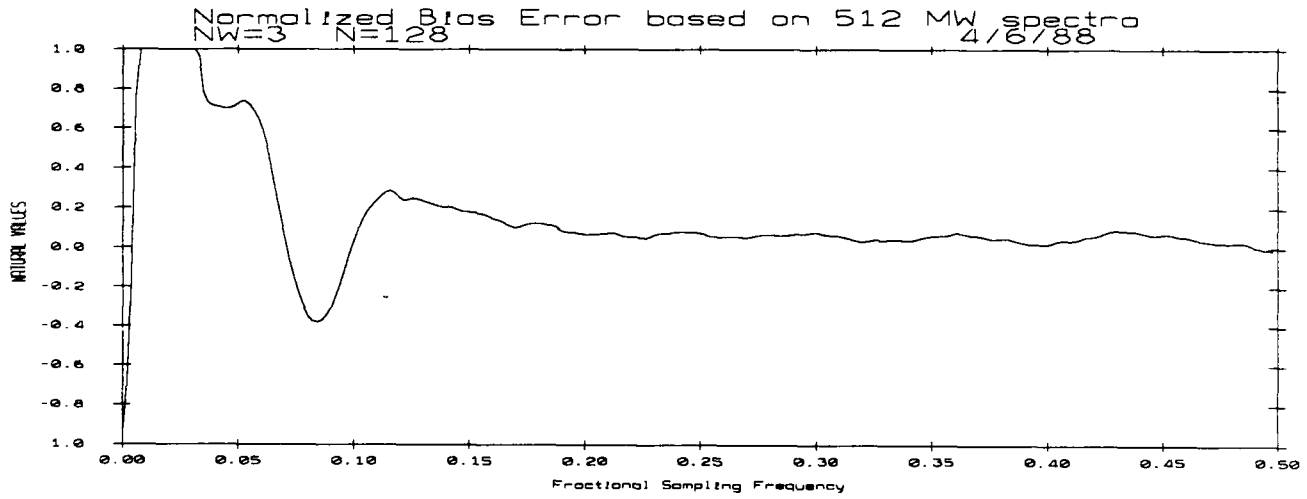
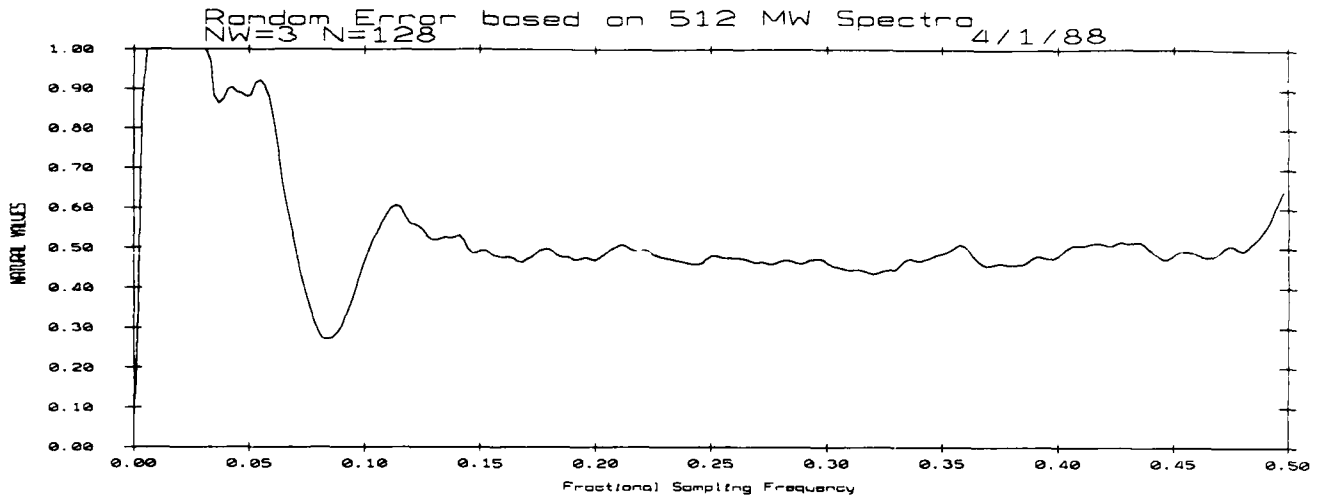


Figure 7.3.3 Normalized random error ϵ_r

Figure 7.3.4 Normalized bias error ϵ_b

Figure 7.3.5 Normalized rms error ϵ_{rms}

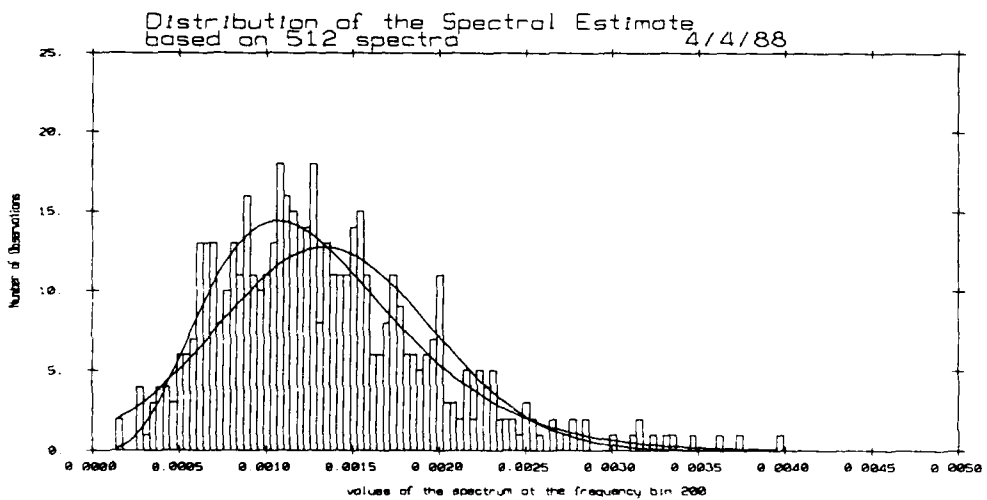
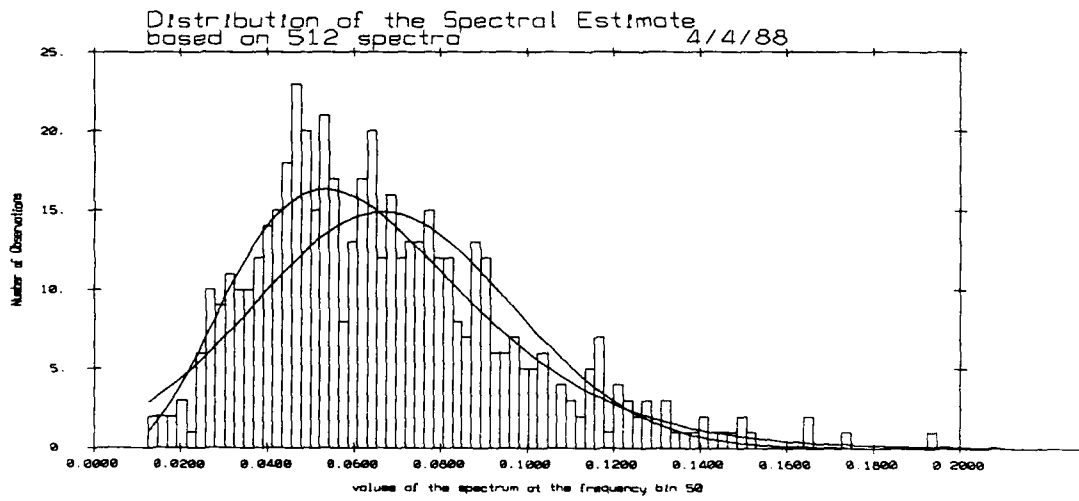
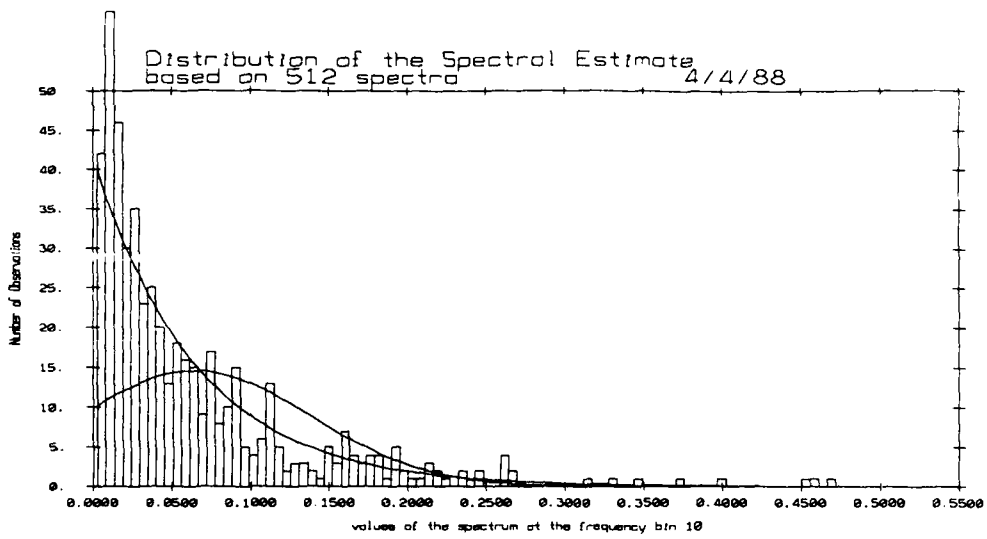


Figure 7.3.6 Sample histogram at the normalized frequency 10/512 overlaid with fitted Gaussian and χ^2_2 distributions

Figure 7.3.7 Sample histogram at the normalized frequency 50/512 overlaid with fitted Gaussian and χ^2_{10} distributions

Figure 7.3.8 Sample histogram at the normalized frequency 200/512 overlaid with fitted Gaussian and χ^2_{10} distributions

7.4. MW Estimate On 576 Points with $NW=4$

To have a more complete picture of the MW estimation capabilities, 512 MW estimates based on the same 576 points as in §6 (FFT estimates) are computed. The Fourier transform are performed on 2048 points.

The overlaid spectra are plotted on Figure 7.4.1 and the mean and envelope of the estimate are plotted on Figure 7.4.2. One can already see that the MW method, in this case, resolves well the spectrum with a variance control similar to the FFT estimates of §6.

The random error ϵ_r , plotted on Figure 7.4.3, is essentially equal to 0.4 with a peak to 2.8 at low frequency. The bias error ϵ_b , plotted on Figure 7.4.4, varies between 0 and 0.1 with an extremum down to -0.1 corresponding to the local maximum of the spectrum (shipping bump) and with a maximum of value 2.85 at low frequency. The rms error ϵ_{rms} is dominated by the random error as can be seen on Figure 7.4.5 ; it varies around 0.4 with a peak value at low frequency of 4. These errors are comparable to the errors obtained with the FFT based estimates (§6).

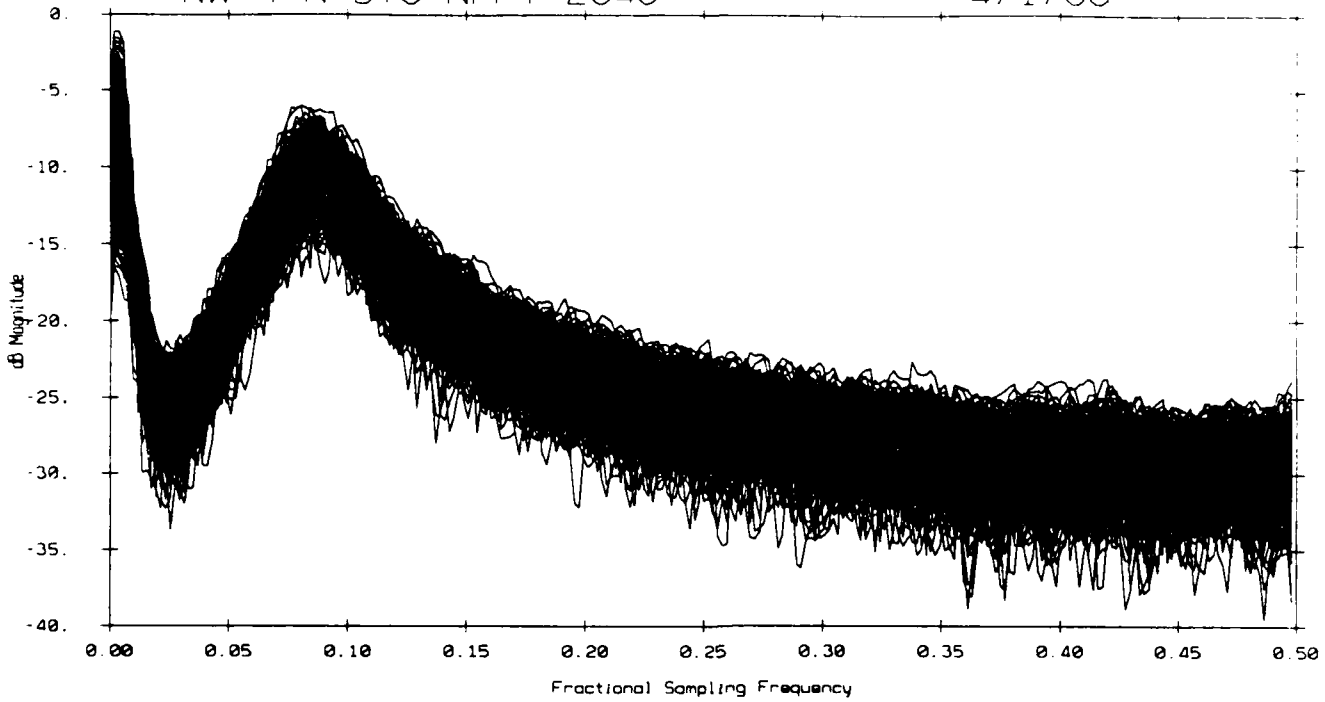
The distributions of the spectral estimates at the pre-selected frequencies (§2) are plotted on Figure 7.4.6, 7.4.7, 7.4.8. The maximum number of degrees of freedom one can expect is 16, since 8 windows are used ($NW=4$). As before chi-square distributions are fitted to the sample histograms at the $\alpha = 0.05$ level of significance, the numbers of degrees of freedom are at the normalized frequencies 10/512, 50/512 and 200/512 respectively 12, 16 and 14.

Normalized Errors			
	ϵ_r	ϵ_b	ϵ_{rms}
characteristic Value	0.4	0.1	0.4
Maximum Value	2.8	2.8	4

Approximate Number of Degrees of Freedom			
Normalized Frequency	10/512	50/512	200/512
Degrees of Freedom	12	16	14

512 MW based Spectra
NW=4 N=576 NFFT=2048

4/1/88



Mean and Envelope of 512 MW based Spectra
NW=4 N=576

4/5/88

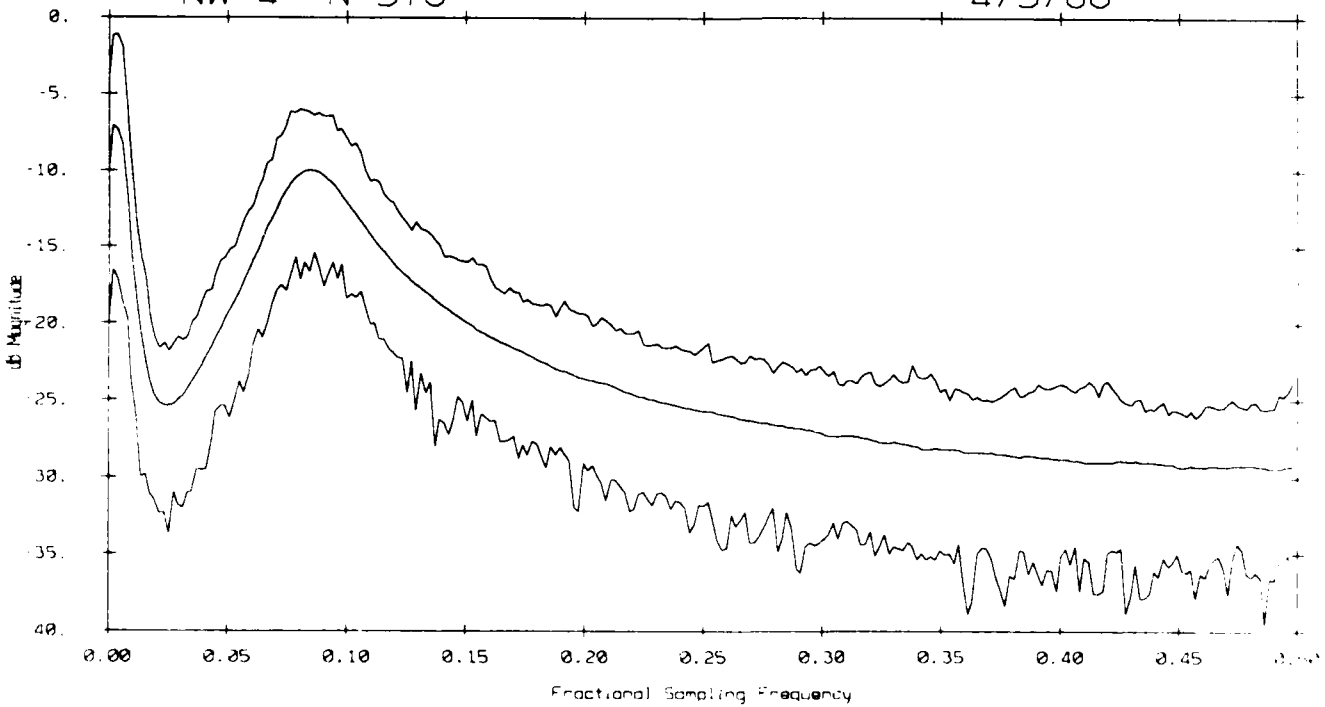


Figure 7.4.1 512 overlaid spectral densities computed by the MW method on 576 points with a time bandwidth product NW of 4

Figure 7.4.2 Mean and envelope of the spectral densities

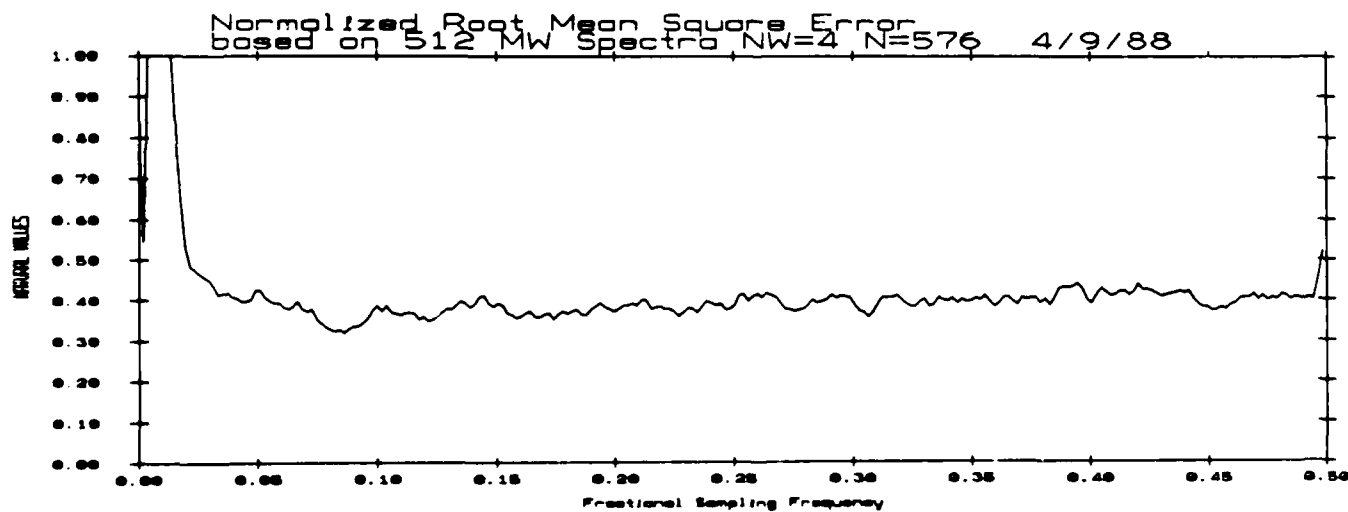
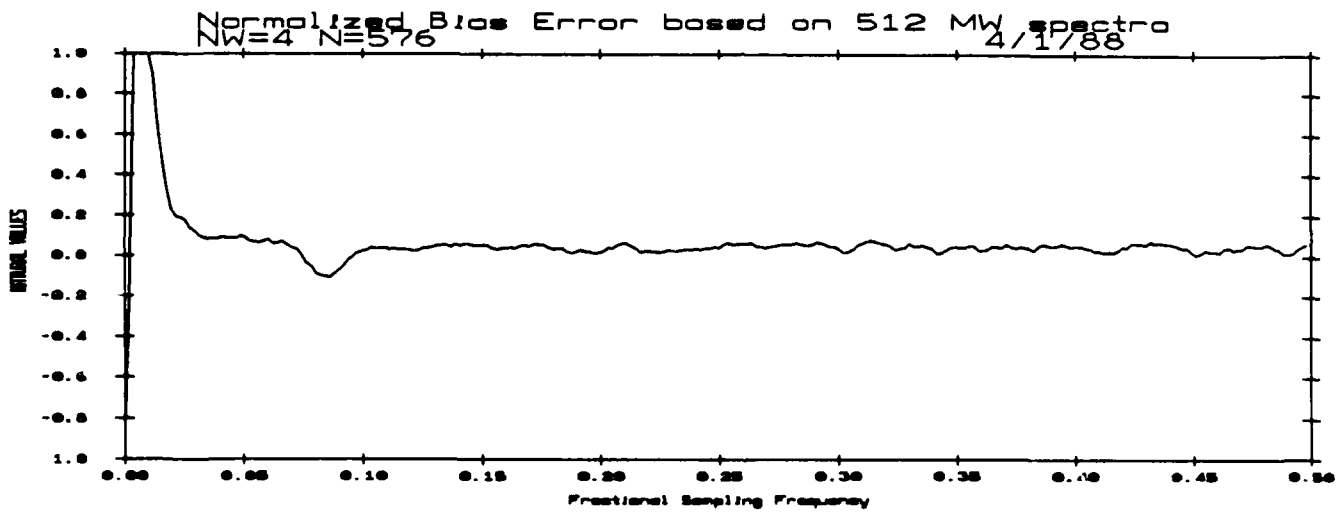
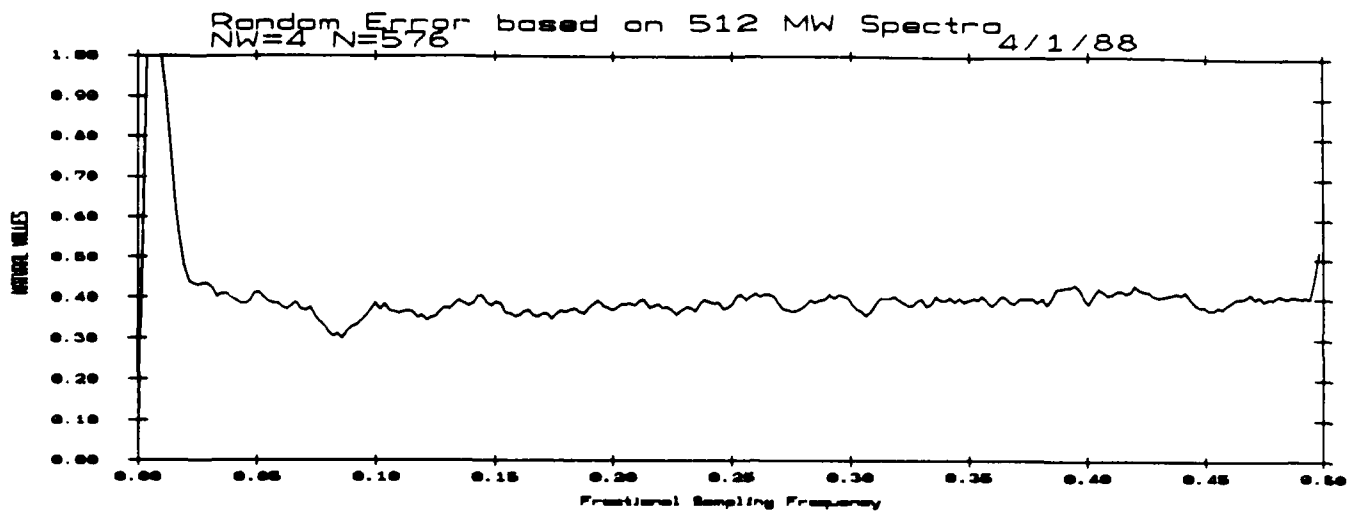


Figure 7.4.3 Normalized Random error ϵ_r

Figure 7.4.4 Normalized bias error ϵ_b

Figure 7.4.5 Normalized rms error ϵ_{rms}

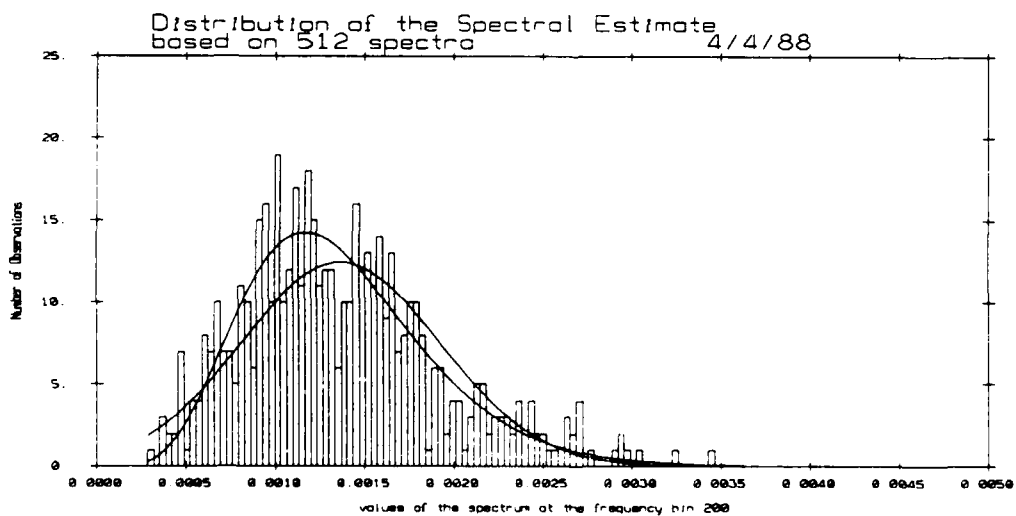
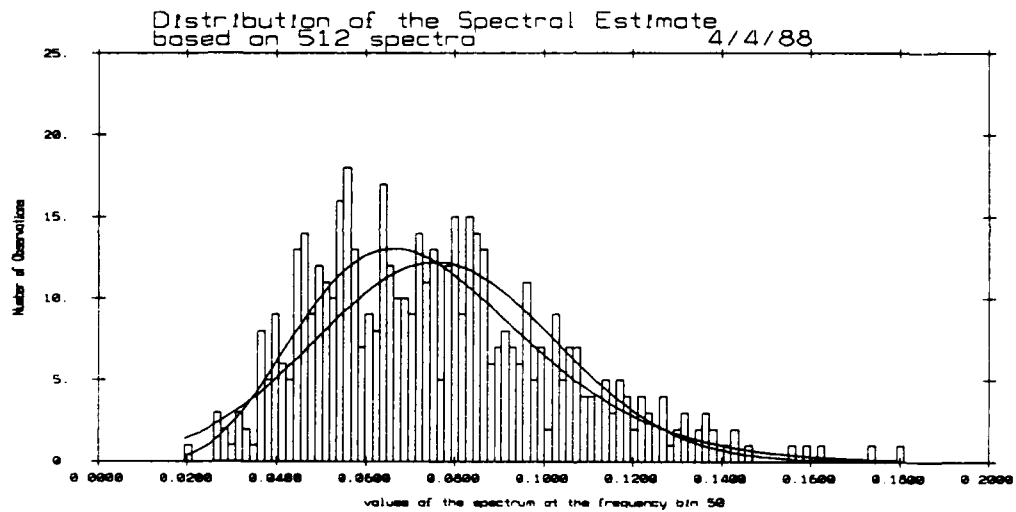
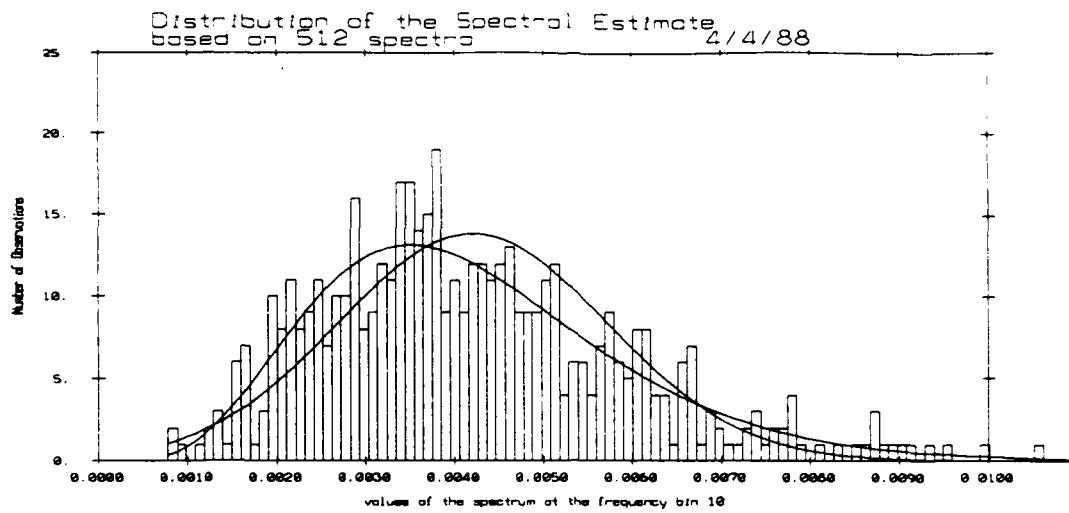


Figure 7.4.6 Sample histogram at the normalized frequency 10/512 overlaid with fitted Gaussian and χ^2_{12} distributions

Figure 7.4.7 Sample histogram at the normalized frequency 50/512 overlaid with fitted Gaussian and χ^2_{16} distributions

Figure 7.4.8 Sample histogram at the normalized frequency 200/512 overlaid with fitted Gaussian and χ^2_{14} distributions

8. Maximum Likelihood Estimate

8.1. Order Selection

As noted in §4, the Maximum Likelihood spectral estimate of order p is an average of the AR spectral estimates of order smaller or equal to p . The order selection for the MLM method can be thought similar to the order selection of an AR spectral estimate.

A way to select an AR model order is to look at the residual energy between the data and the modelled data. Such residual decreases with the model order and eventually settles. Such an analysis was carried out with 128 data points extracted from the "ambient noise" data set : the residual energy is plotted on Figure 8.1.1.

The residual seems to level off for an AR model order of 16 which should be a good choice for the maximum likelihood spectral estimate. To have more information in the comparison between the MW estimates and the MLM estimates, the simulation is carried out for orders p equal to 8, 16 and 32.

RESIDUAL ENERGY VERSUS AR MODEL ORDER

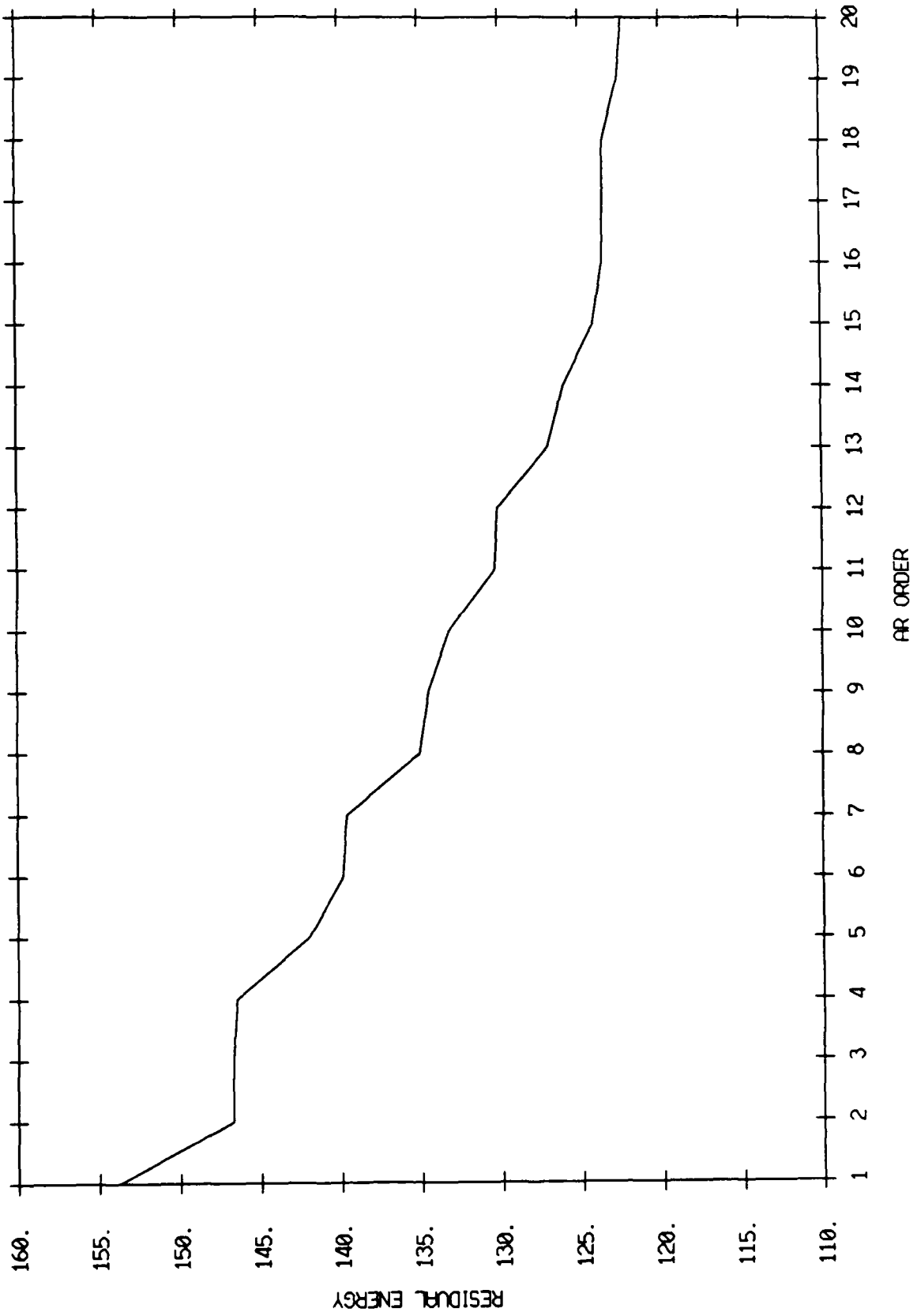


Figure 8.1.1 Residual energy as a function of the AR model order on one of the 128 point long sequence

8.2. MLM Estimate of order 8 On 128 points

512 spectra are computed on the same 128 data points as the MW spectral estimates of §2 and §3. The order p of the autocorrelation matrix R_p is 8. The data are well behaved since none of the autocorrelation matrix was singular. The Fourier Transforms that implements the method are done on 256 points.

The overlaid spectral density realizations obtained by the MLM method are plotted on Figure 8.2.1. The mean and envelope of the estimates are plotted on Figure 8.2.2. The selection of a low order produces a good variance control (the spectral estimates are very smooth), but a poor resolution. The dip at the normalized frequency 0.0625 is not resolved and the shape of the spectrum does not fit the theoretical one. This lack of resolution could be expected since the dip corresponds to the moving average part of the ARMA (5,4) process used to create the "ambient noise" data. There is a large scatter of the estimates at low frequency.

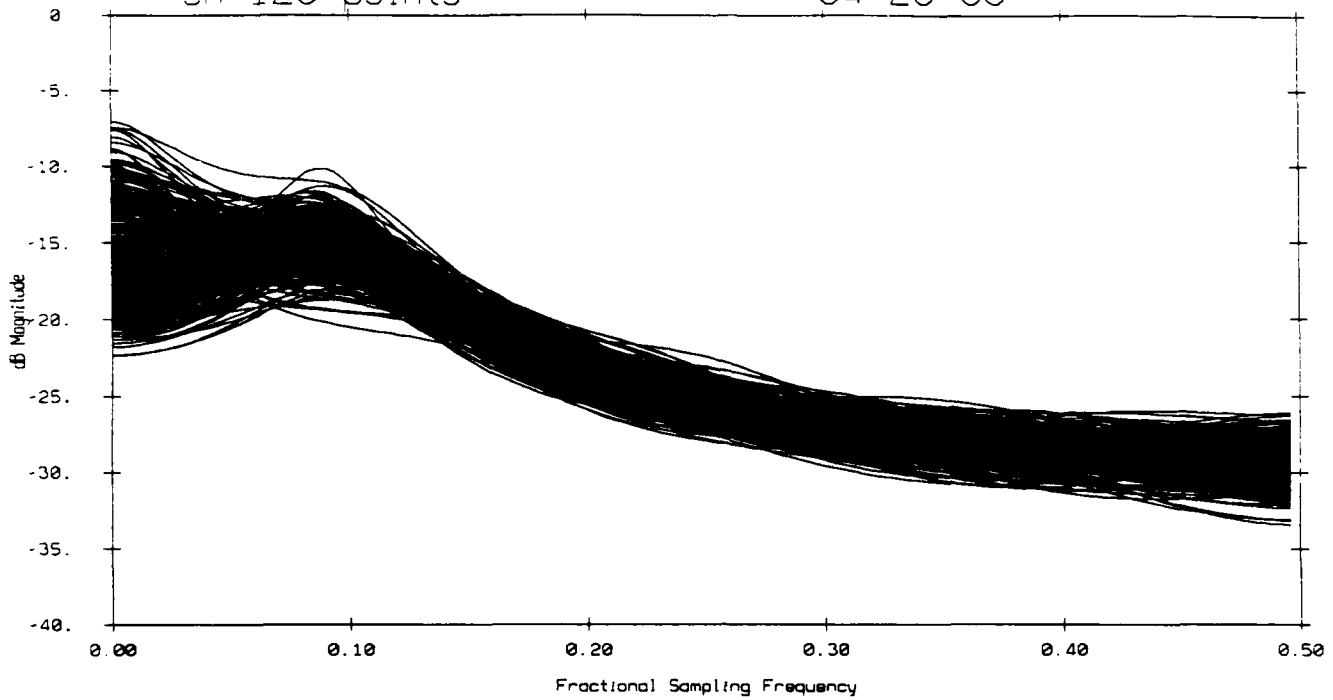
The random error ϵ_r , plotted on Figure 8.2.3, is varying below 0.3 at intermediate and high frequency with a maximum value of 7.5 at low frequency. The bias error ϵ_b , plotted on Figure 8.2.4, is generally below 0.2 except at low frequency where it goes up to 11. The rms error ϵ_{rms} , plotted on Figure 8.2.5, stays below 0.3 in most the frequency band with a peak value, at the power spectrum local maximum (shipping bump), of 0.7. The highest value of ϵ_{rms} is 13.6 at low frequency.

The distributions and sample histograms at the pre-selected frequencies (§2) are plotted on Figures 8.2.6, 8.2.7 and 8.2.8. The low frequency (10/512) histogram look like the ones of §7.2 or §7.3 (MW estimate with NW equal 2 or 3). Any chi-square distribution of any order is rejected at the $\alpha=0.05$ level of significance. At the frequency 50/512, the fitted chi-square accepted by the goodness of fit test has 16 degrees of freedom. At high frequency (200/512), the distribution is essentially a Gaussian distribution : the fitted chi-square has 36 degrees of freedom.

	ϵ_r	ϵ_b	ϵ_{rms}
Characteristic Value	0.3	< 0.2	0.3
Maximum Value	7.5	11	13.6

Normalized Frequency	10/512	50/512	200/512
Degrees of Freedom	< 2	16	36

512 MLM estimates of order 8
on 128 points 04-28-88



Mean and Envelope of 512 MLM estimates of order 8
on 128 points 04-25-88

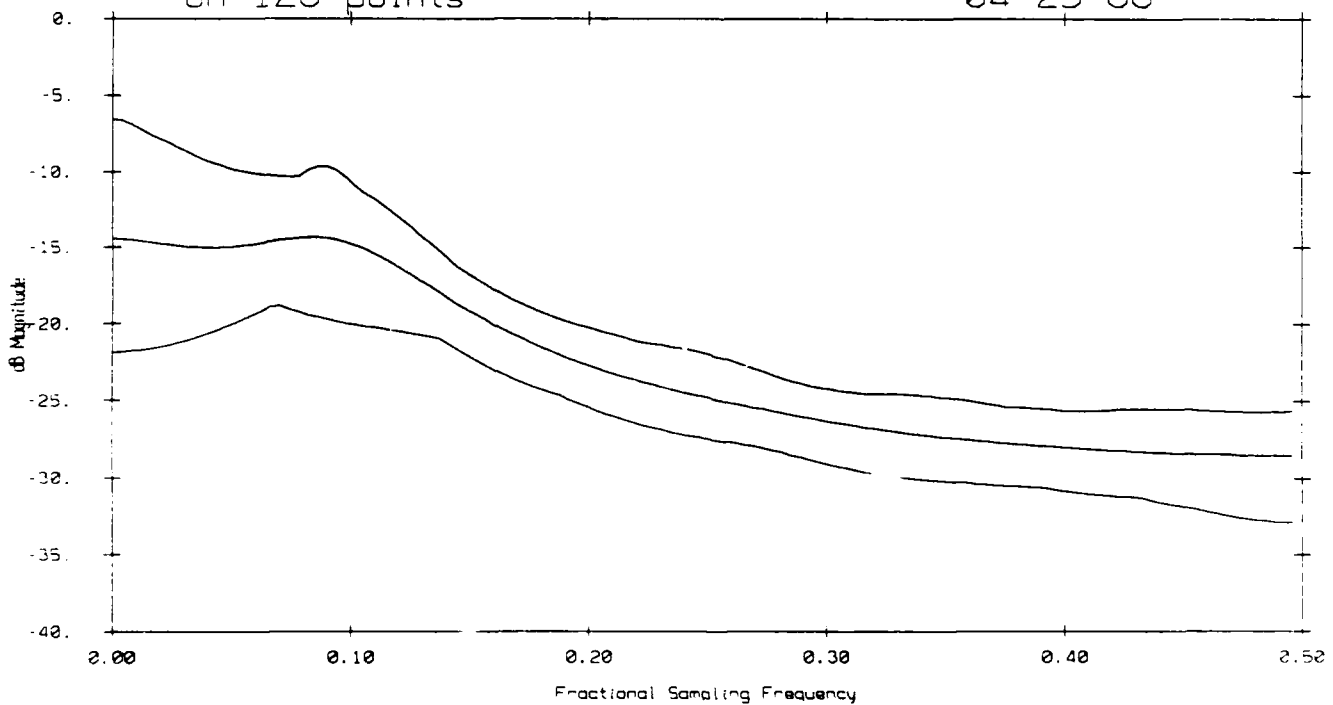


Figure 8.2.1 512 overlaid spectral densities computed by the MLM method on 128 points with an order p of 8

Figure 8.2.2 Mean and envelope of the spectral densities

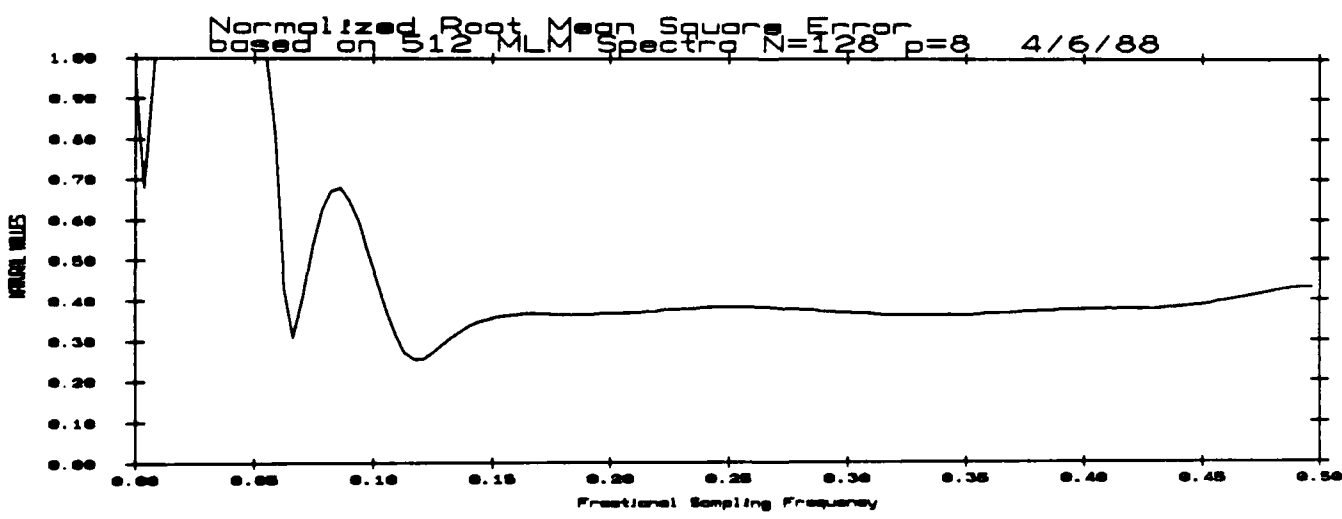
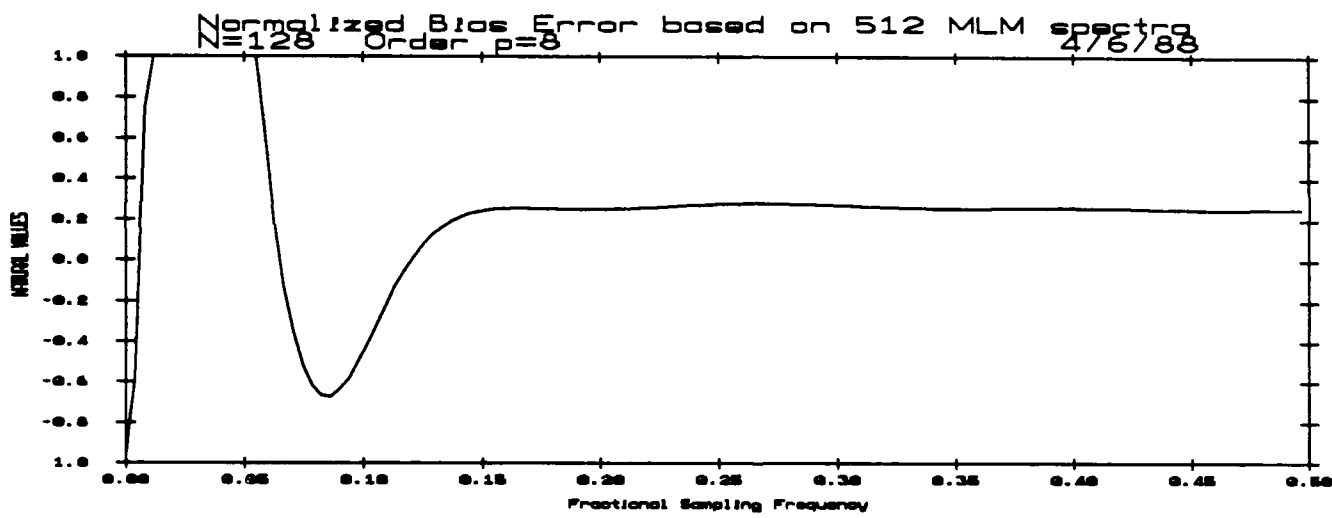
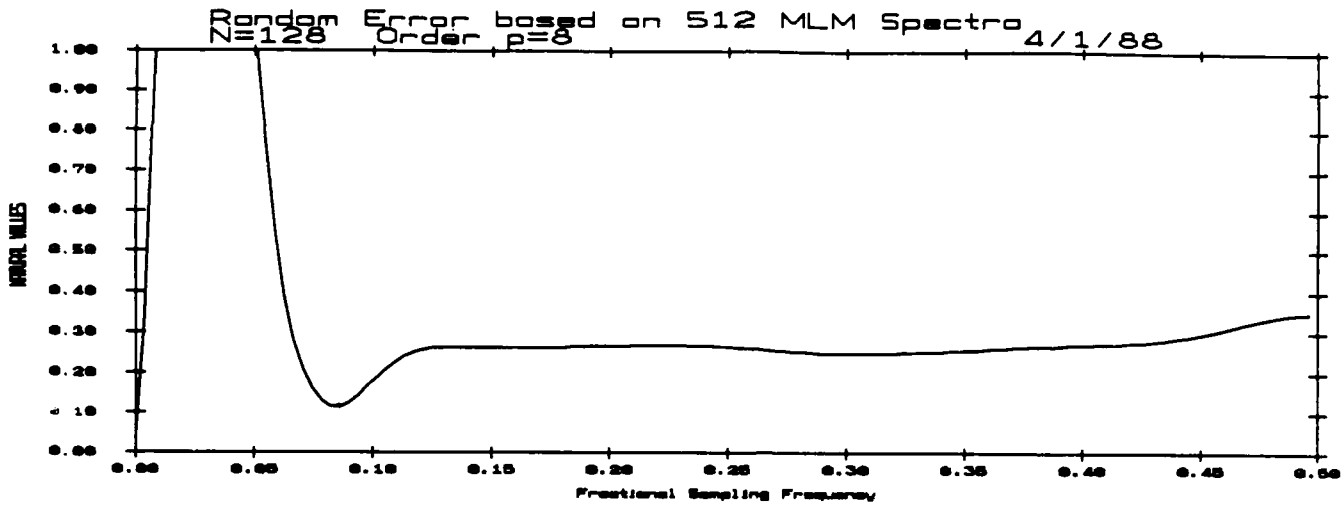


Figure 8.2.3 Normalized random error ϵ_r

Figure 8.2.4 Normalized bias error ϵ_b

Figure 8.2.5 Normalized rms error ϵ_{rms}

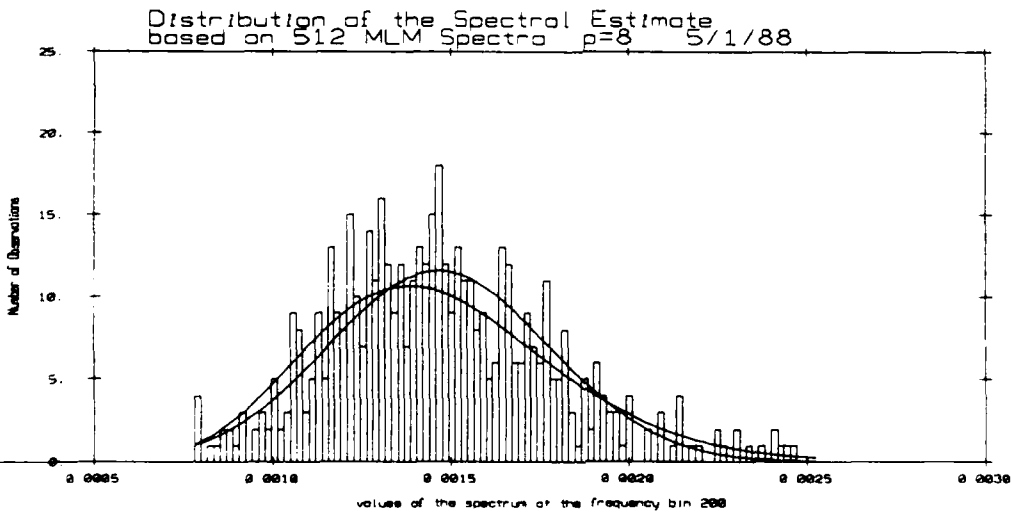
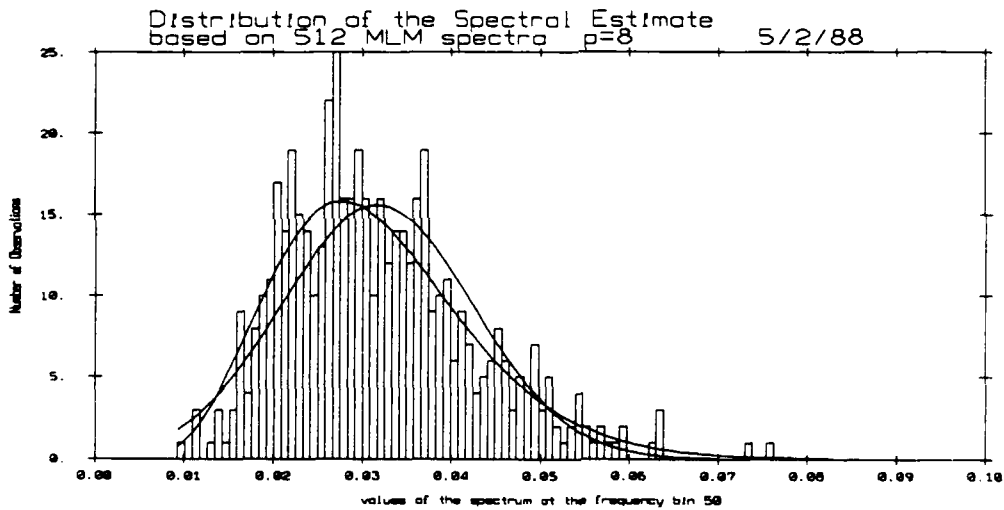
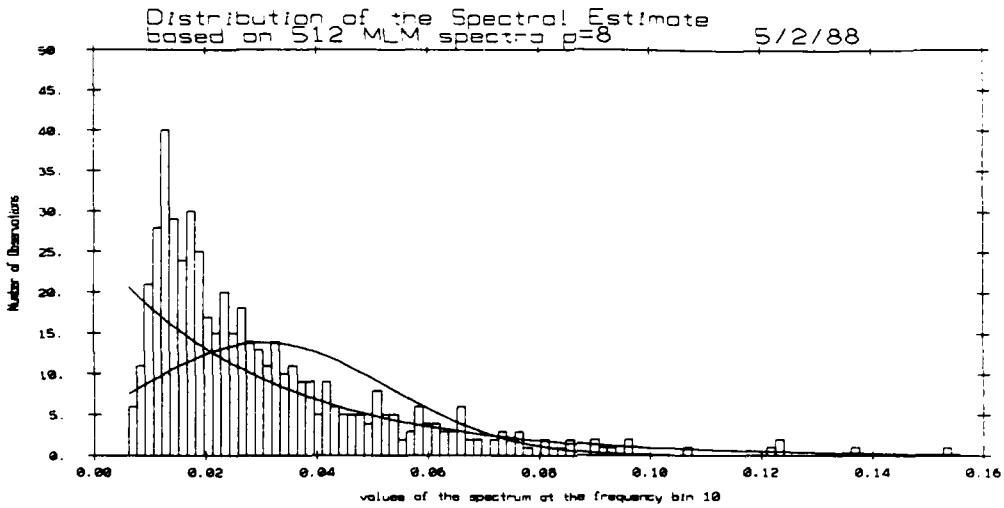


Figure 8.2.6 Sample histogram at the normalized frequency 10/512 overlaid with fitted Gaussian and χ^2_2 distributions

Figure 8.2.7 Sample histogram at the normalized frequency 50/512 overlaid with fitted Gaussian and χ^2_{16} distributions

Figure 8.2.8 Sample histogram at the normalized frequency 200/512 overlaid with fitted Gaussian and χ^2_{36} distributions

8.3. MLM Estimate of order 16 On 128 Points

The order of the autocorrelation matrix is doubled, p is 16, one expects more resolution and also more variance than in §8.2. 512 spectral estimates based on the usual 128 points of the "ambient noise" sequence are computed. The Fourier transforms implementing the MLM method are performed on 256 points.

The overlaid spectra are plotted on Figure 8.3.1. The mean and envelope of the estimates are plotted on Figure 8.3.2. One can already recognize an improvement in the resolution of the estimate with respect to §8.2, for a limited variance increase. There is still a large scatter of the spectral estimates near DC.

The random error ϵ_r , plotted on Figure 8.3.3, is essentially equal to 0.3 except at high frequency where it increases up to 0.4, and at low frequency where it peaks up to 3.5. The random error has a minimum at the power spectrum local maximum (shipping bump) with a value of 0.2.

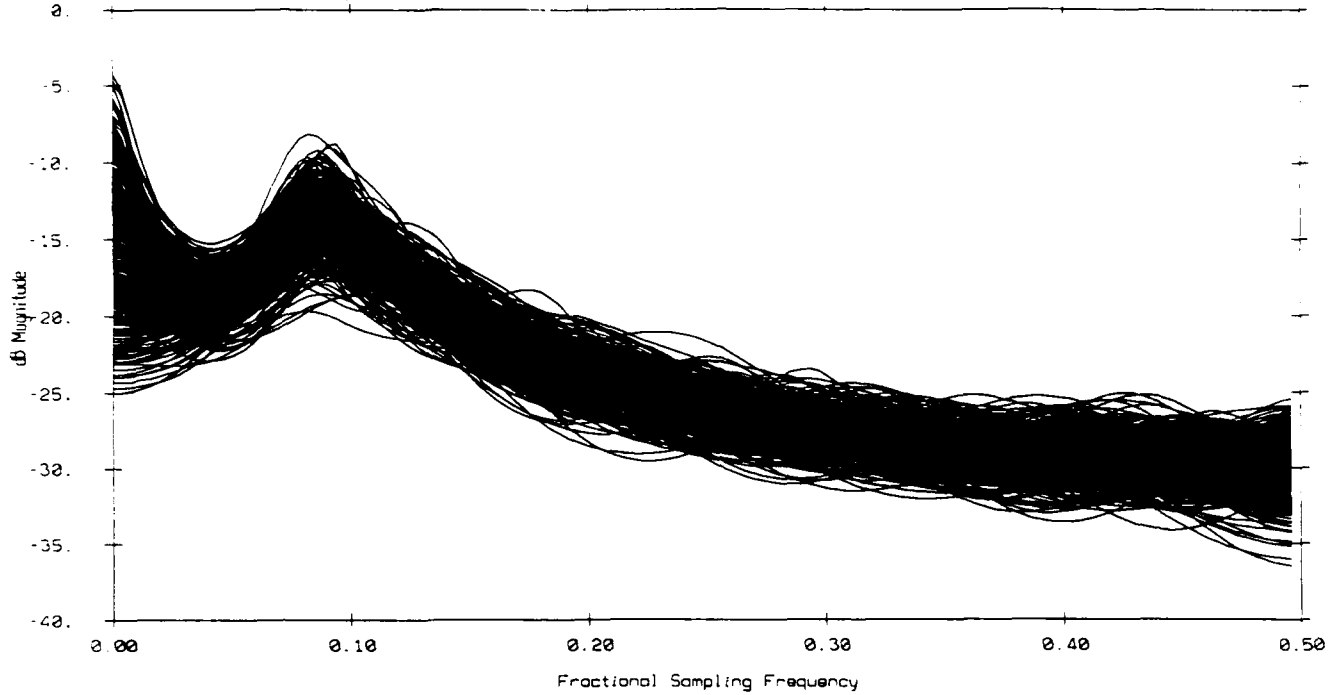
The bias error ϵ_b , plotted on Figure 8.3.4, is essentially zero with two extrema, the first one at low frequency with value equal to 6.2, and the second one at the power spectrum local maximum (shipping bump) with a value equal to -0.6. The rms error is plotted on Figure 8.3.5, it varies as in §8.2 around 0.3 except at high frequency where it increases to 0.4 and at low frequency where it has a maximum value of 7.

The distributions and sample histograms at the pre-selected frequencies (§2) are plotted on Figure 8.3.6, 8.3.7, 8.3.8. Chi-square distributions are fitted to the sample histograms at the $\alpha = 0.05$ level of significance with a number of degrees of freedom equal to 6, 12 and 20 for the respective normalized frequencies 10/512, 50/512 and 200/512. Although the variance only increases slightly, the order selection has an impact on the distributions.

Table 8.3.1			
Normalized Errors			
	ϵ_r	ϵ_b	ϵ_{rms}
Characteristic Value	0.3	≈ 0	0.3
Maximum Value	3.5	6.2	7

Table 8.3.2			
Approximate Number of Degrees of Freedom			
Normalized Frequency	10/512	50/512	200/512
Degrees of Freedom	6	12	20

512 MLM estimates of order 16
on 128 points 04-27-88



Mean and Envelope of 512 MLM estimates of order 16
on 128 points 04-28-88

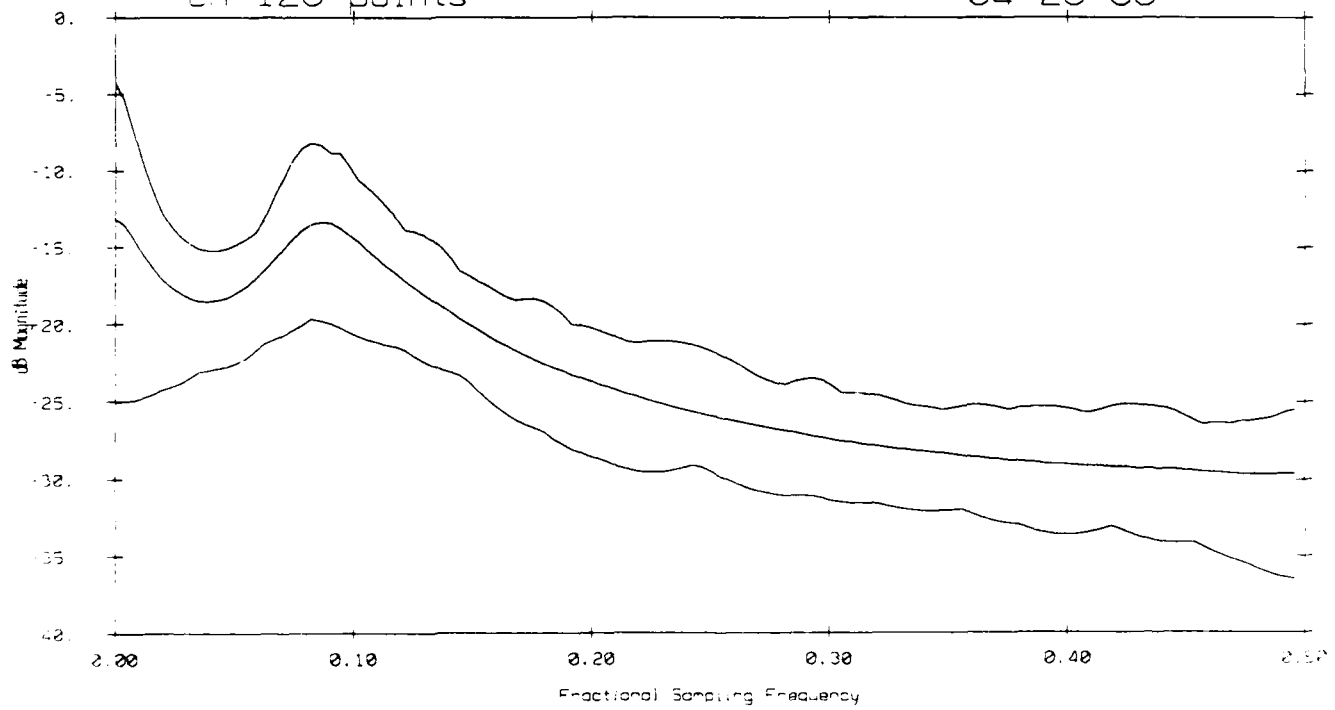


Figure 8.3.1 512 overlaid spectral densities computed by the MLM method on 128 points with an order p equal 16

Figure 8.3.2 Mean and envelope of the spectral densities

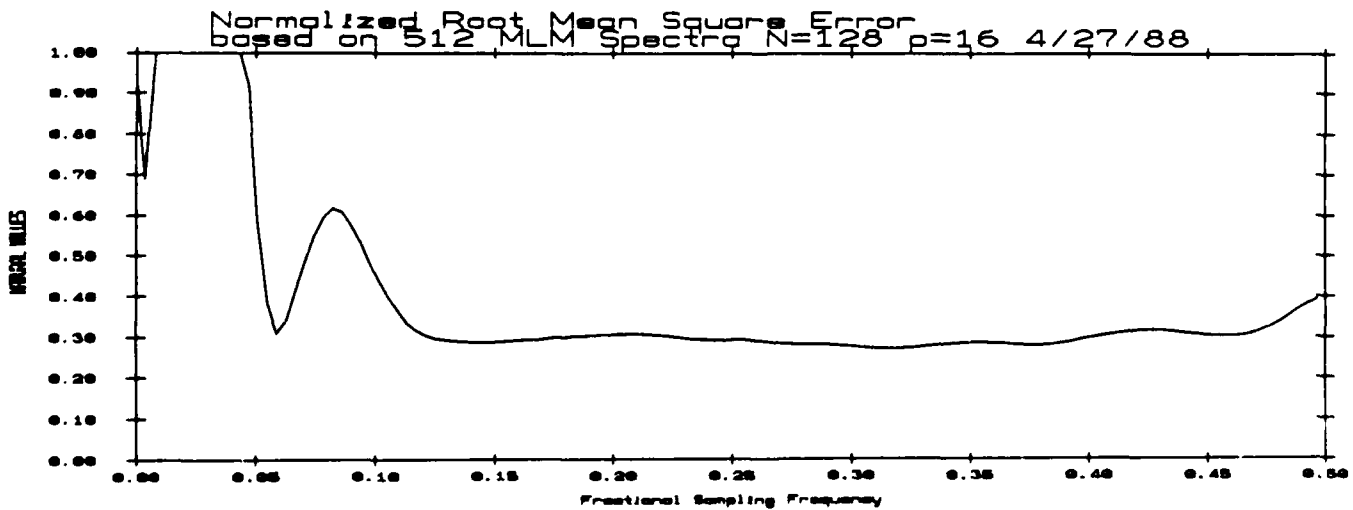
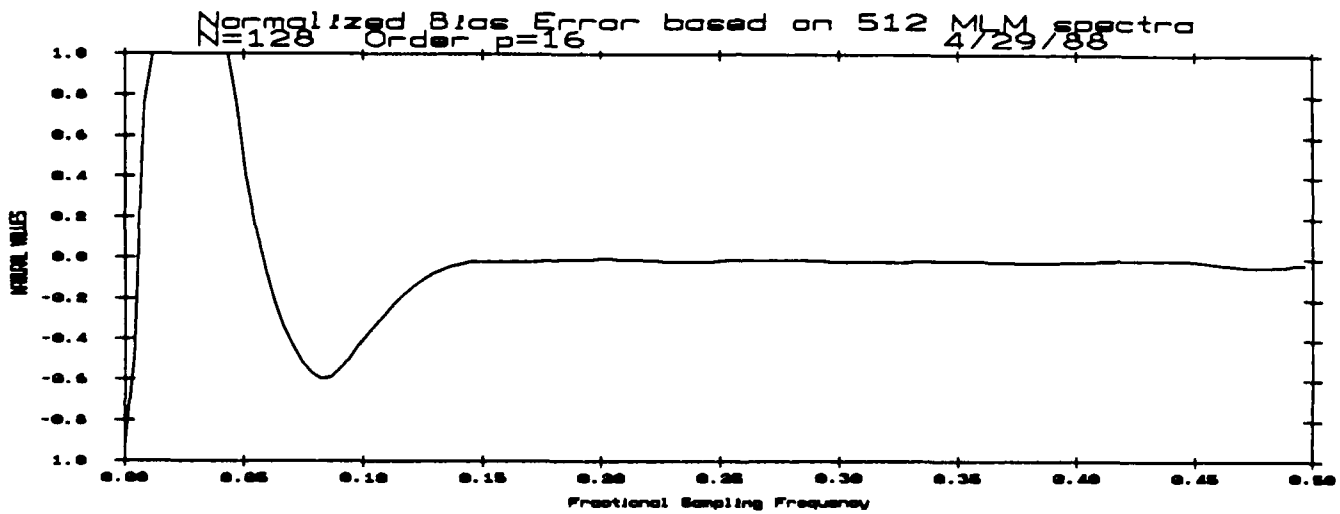
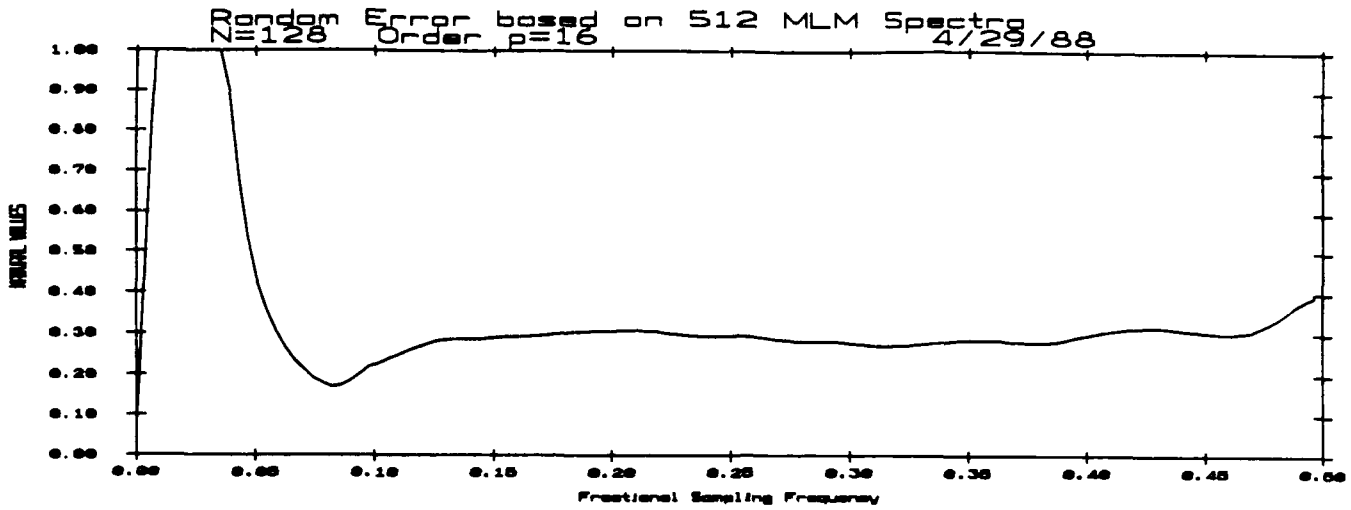


Figure 8.3.3 Normalized random error ϵ_r

Figure 8.3.4 Normalized bias error ϵ_b

Figure 8.3.5 Normalized rms error ϵ_{rms}

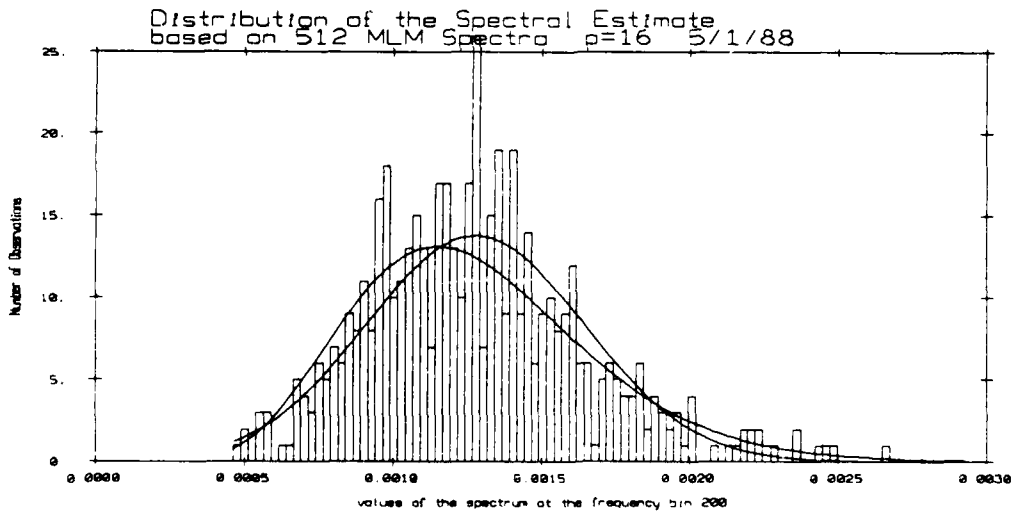
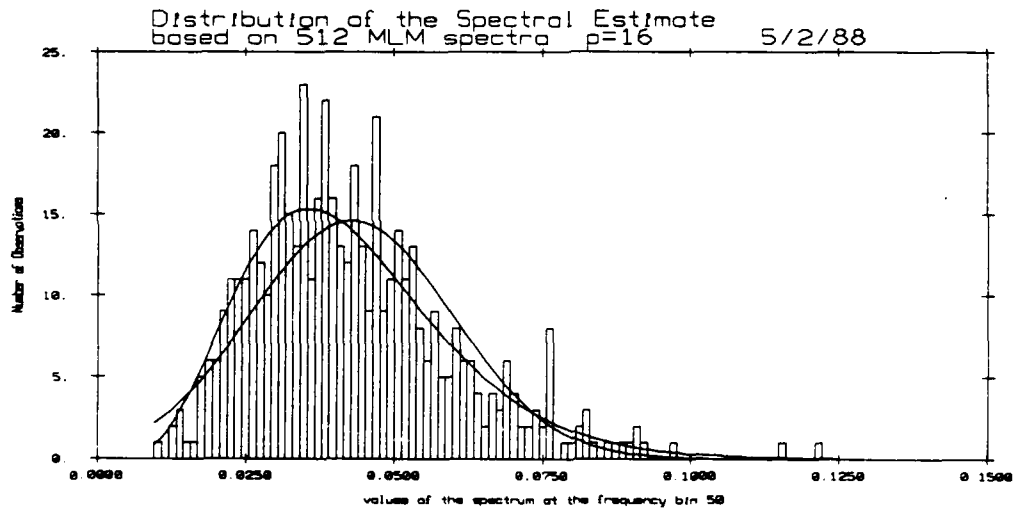
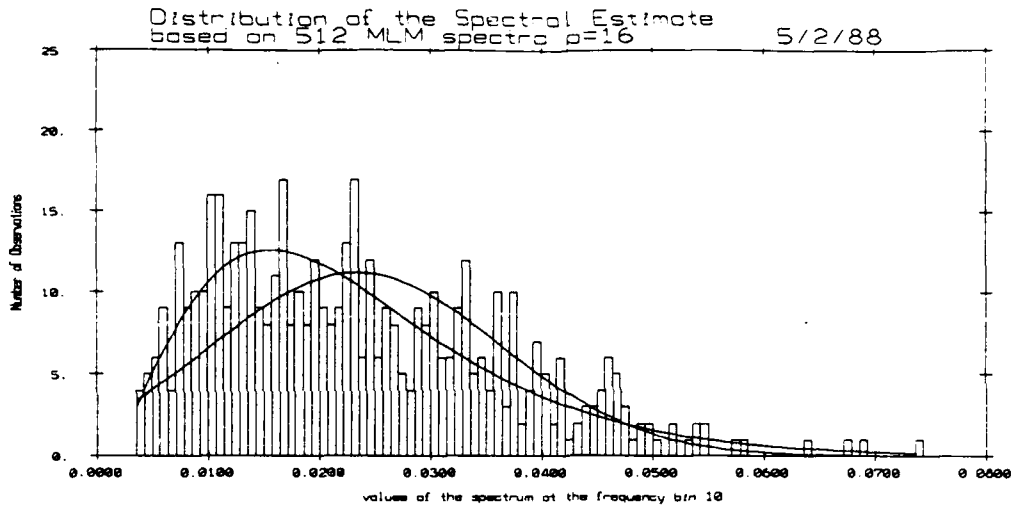


Figure 8.3.6 Sample histogram at the normalized frequency 10/512 overlaid with fitted Gaussian and χ^2_6 distributions

Figure 8.3.7 Sample histogram at the normalized frequency 50/512 overlaid with fitted Gaussian and χ^2_{12} distributions

Figure 8.3.8 Sample histogram at the normalized frequency 200/512 overlaid with fitted Gaussian and χ^2_{20} distributions

8.4. MLM Estimate Of Order 32 On 128 Points

The order p of the autocorrelation matrix is now 32. Once again, the 512 spectral estimates based on the same 128 data points are computed. One expects more resolution and more variance than in § 8.3.

The overlaid spectra are plotted on Figure 8.4.1. The mean and envelope of the estimates are plotted on Figure 8.4.2. One visually checks an increase in the resolution of the estimate and its variability.

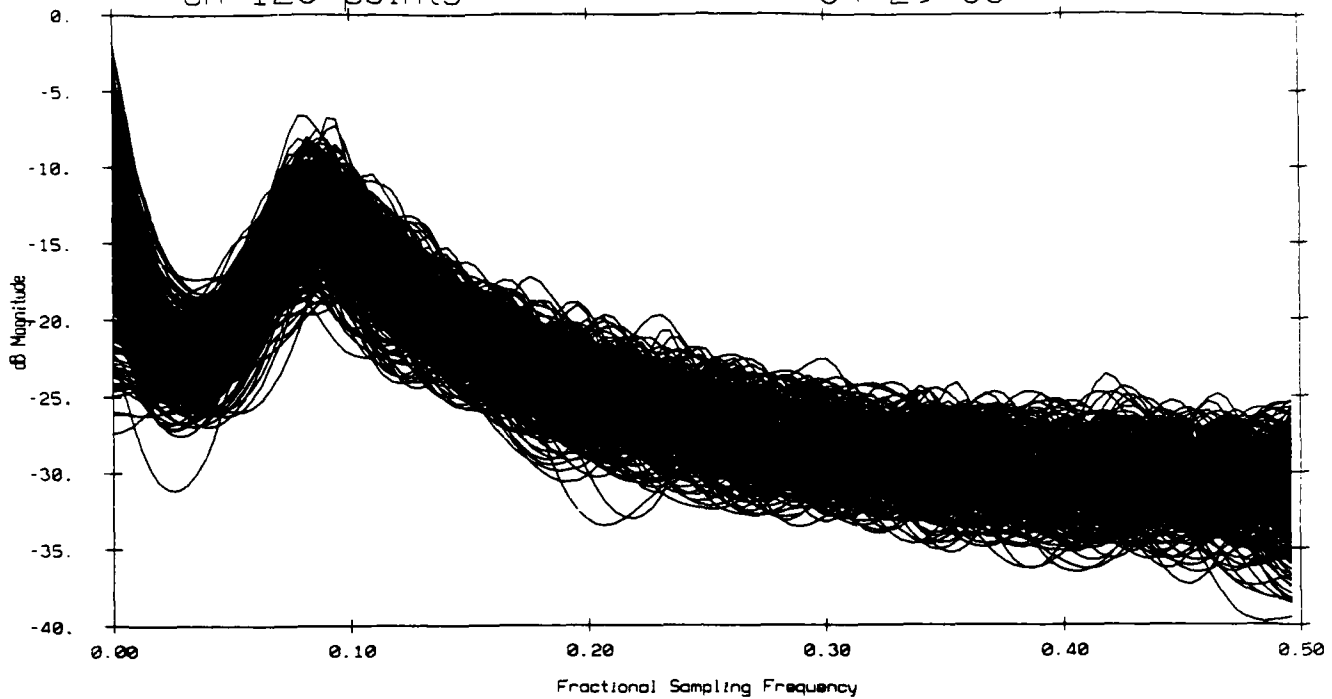
The random error ϵ_r , plotted on Figure 8.4.3, varies below 0.4 except at high frequencies where it increases up to 0.48 and at low frequency where it peaks up to 1.6. As before there is a minimum value of 0.25 that corresponds to the power spectrum local maximum (shipping bump). The bias error ϵ_b , plotted on Figure 8.4.4, varies around -0.2 with two peaks, one of value 2 at low frequency and one of value -0.55 at the power spectrum local maximum. The rms error ϵ_{rms} is plotted on Figure 8.4.5, it has a peak at low frequency of 2.5 and then varies between 0.4 and 0.5.

The distributions and sample histograms are plotted on Figures 8.4.6, 8.4.7 and 8.4.8. Although the increase of the order p has a weak impact on the random error, it significantly decreases the number of degrees of freedom of the estimate. As before chi-square distributions were fitted using the chi-square goodness of fit test with a level of significance $\alpha = 0.05$. The number of degrees of freedom are respectively 6, 6, 10 for the normalized frequencies 10/512, 50/512 and 200/512.

Table 8.4.1			
Normalized Errors			
	ϵ_r	ϵ_b	ϵ_{rms}
Characteristic Value	0.4	-0.2	< 0.5
Maximum Value	1.6	2	2.5

Table 8.4.2			
Approximate Number of Degrees of Freedom			
Normalized Frequency	10/512	50/512	200/512
Degrees of Freedom	6	6	10

512 MLM estimates of order 32
on 128 points 04-29-88



Mean and Envelope of 512 MLM estimates of order 32
on 128 points 04-28-88

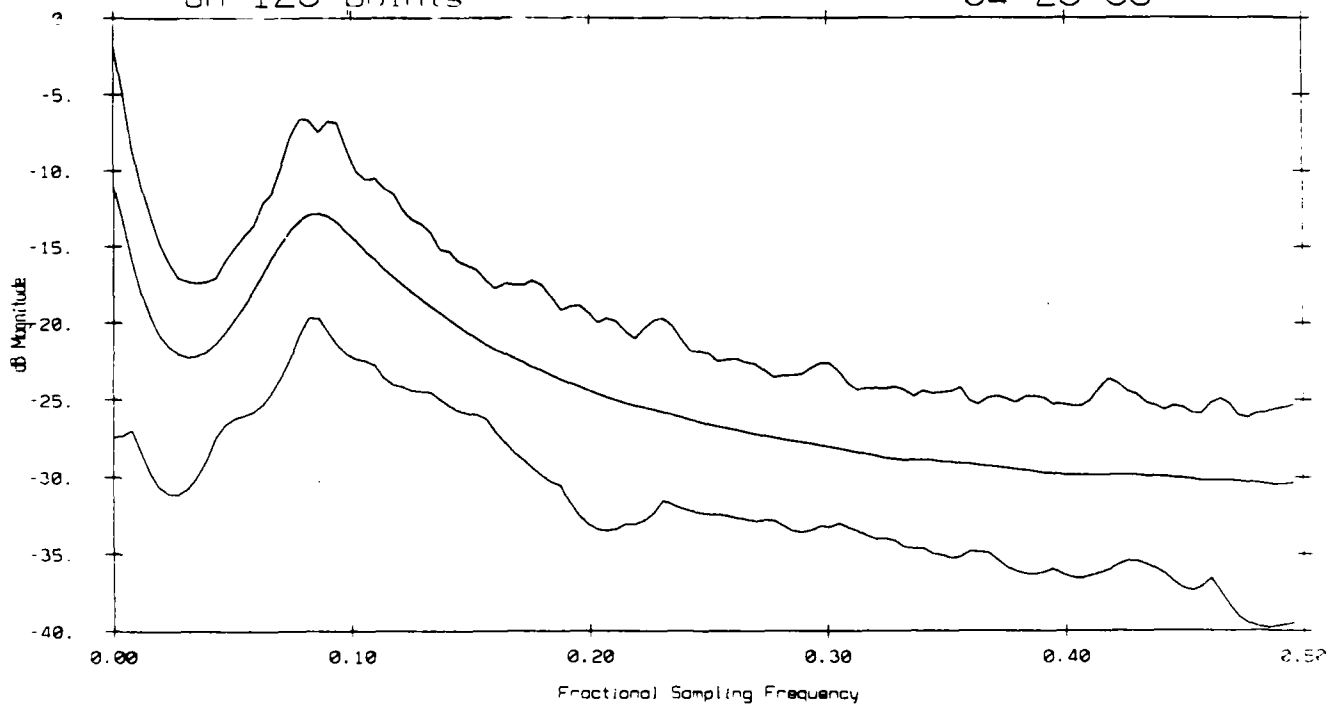


Figure 8.4.1 512 overlaid spectral densities computed by the MLM method on 128 points with an order p of 32

Figure 8.4.2 Mean and envelope of the spectral densities

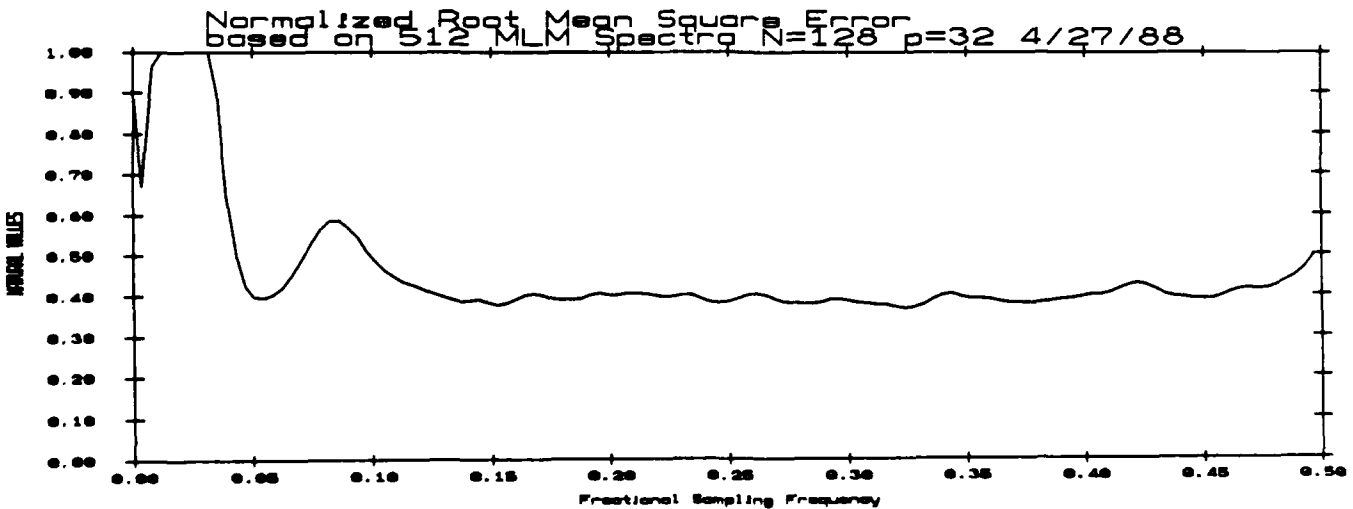
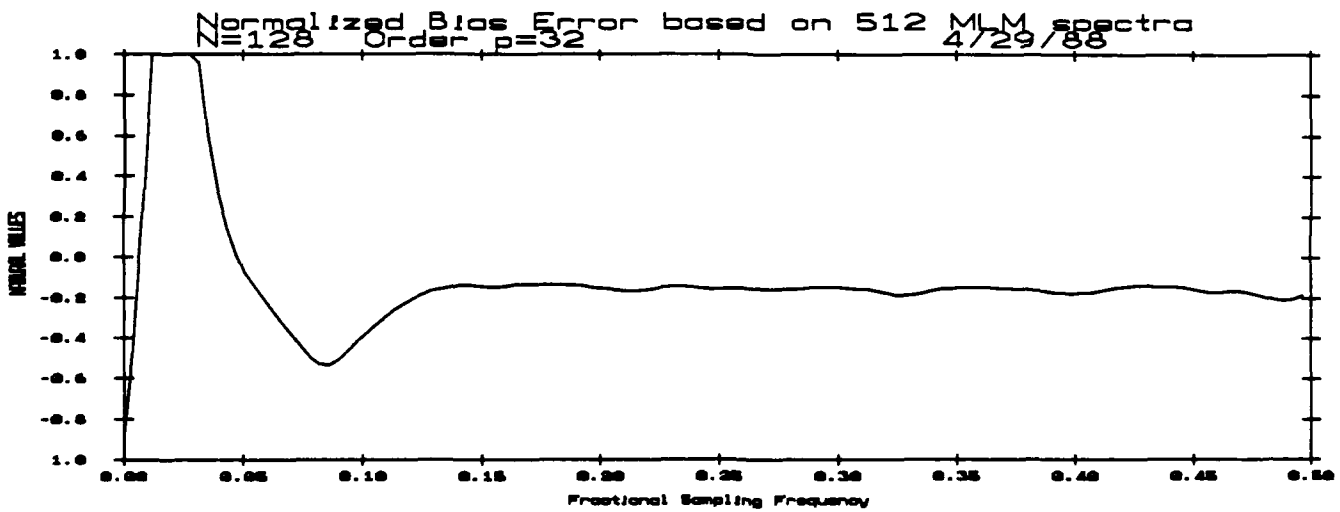
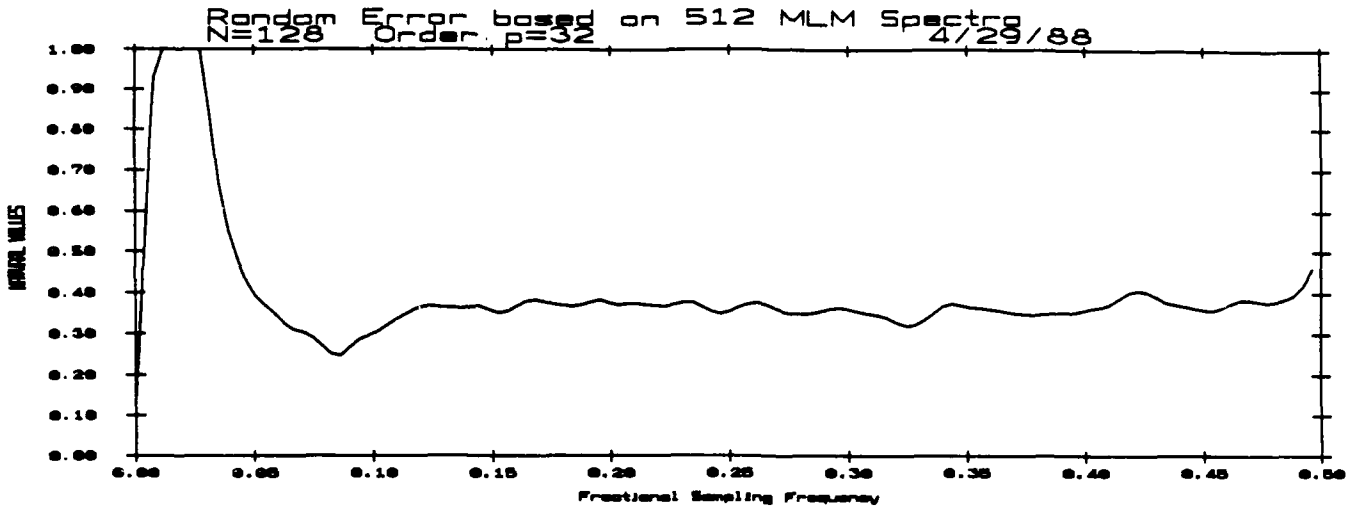


Figure 8.4.3 Normalized random error e_r

Figure 8.4.4 Normalized bias error e_b

Figure 8.4.5 Normalized rms error e_{rms}

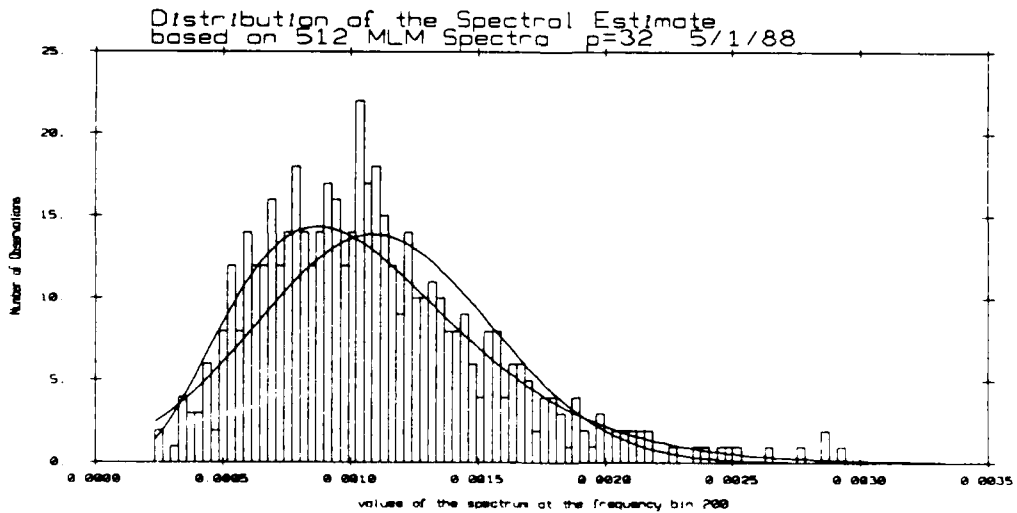
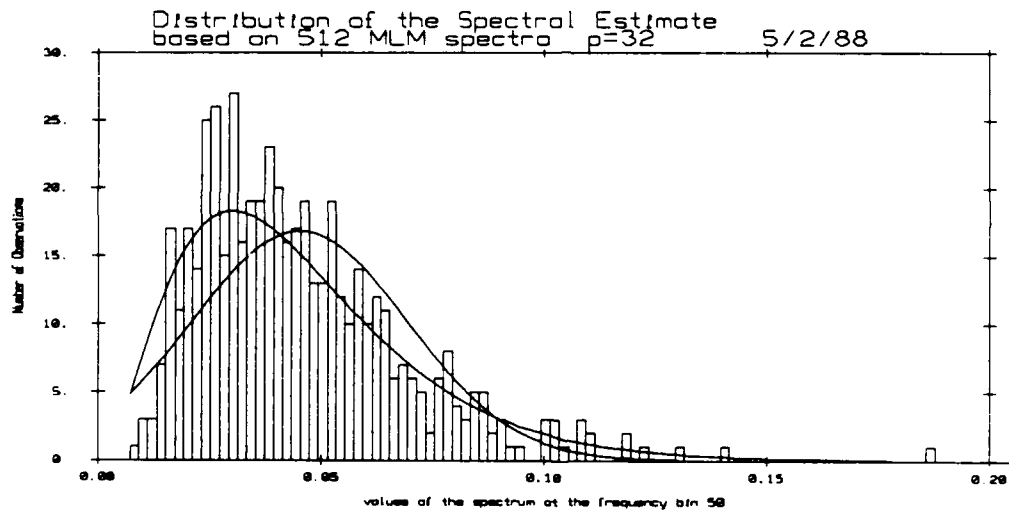
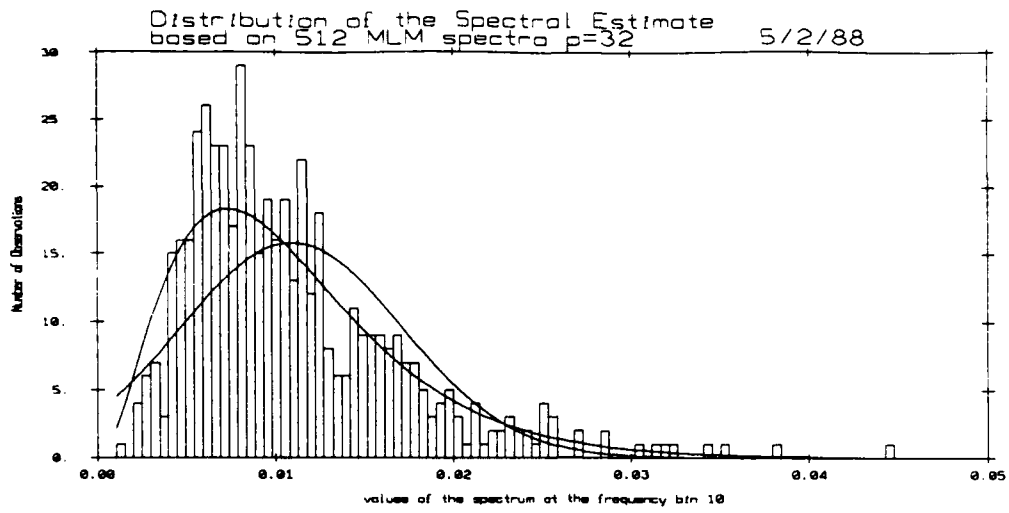


Figure 8.4.6 Sample histogram at the normalized frequency 10/512 overlaid with fitted Gaussian and χ^2_6 distributions

Figure 8.4.7 Sample histogram at the normalized frequency 50/512 overlaid with fitted Gaussian and χ^2_6 distributions

Figure 8.4.8 Sample histogram at the normalized frequency 200/512 overlaid with fitted Gaussian and χ^2_{10} distributions

8.5. MLM Estimate Of Order 32 On 576 points

The MLM spectral estimates are computed on the same 576 points as in §6 and §7.4. More data points are used in the estimation of the autocorrelation matrix of order 32. One expects more resolution and better variance control.

The overlaid spectra are plotted on Figure 8.5.1. The mean and envelope of the estimates are plotted on Figure 8.5.2. One observes a significant decrease in the variability of the estimate.

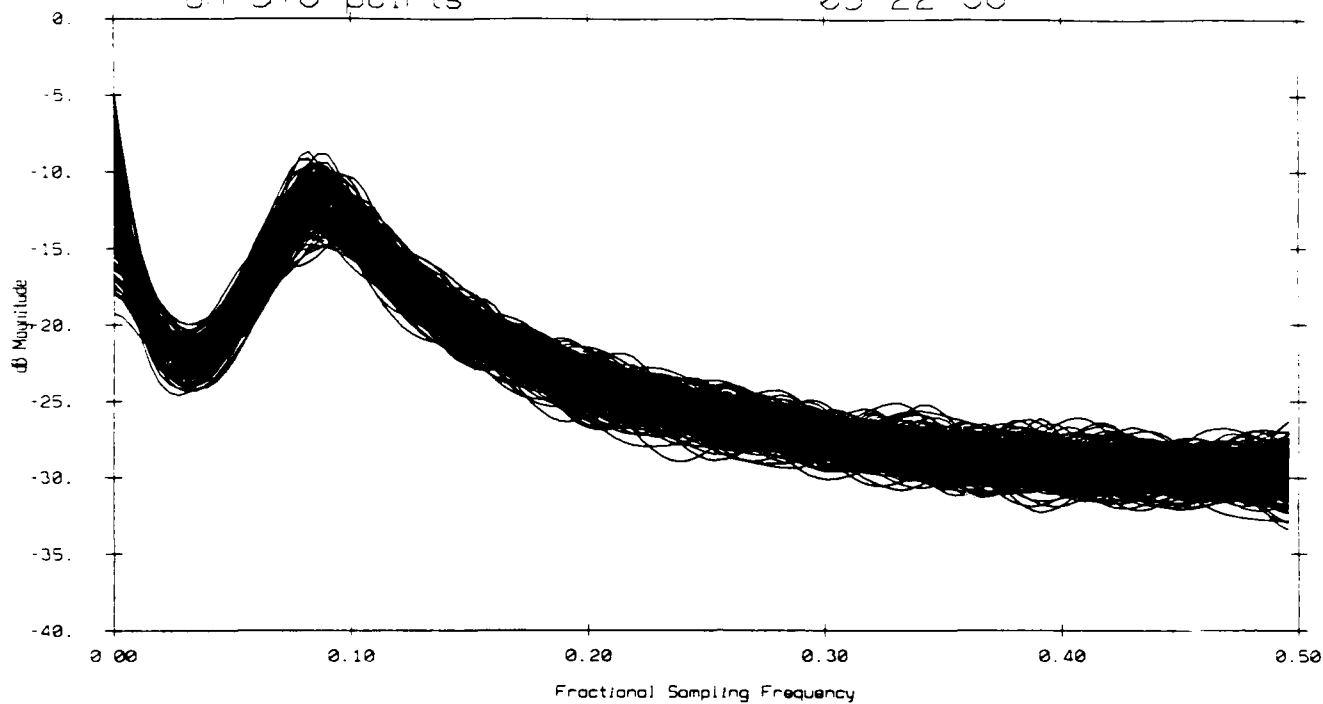
The random error ϵ_r , plotted on Figure 8.5.3 is essentially equal to 0.2 with a low maximum value at 0.54. The bias error ϵ_b , plotted on Figure 8.5.4, is essentially 0 with two extrema, one at the low frequency dip and of value 1.9, the other at the power spectrum local maximum of value -0.4. The rms error ϵ_{rms} is plotted on figure 8.5.5 and varies around 0.2 except at low frequency where it has a peak to 1.8, with a secondary maximum of value 0.4 at the power spectrum local maximum.

The distributions and sample histograms at the pre-selected frequencies (§2) are plotted on Figures 8.5.6, 8.5.7, 8.5.8. Comparison with the fitted Gaussian law indicates that the estimate has a large number of degrees of freedom. At low and high frequencies, an attempt to fit a chi-square distribution shows that the number of degrees of freedom is greater than 40. At intermediate frequency (50/512), the best fit is achieved for a χ^2_{36} (36 degrees of freedom). The goodness of fit test is nevertheless rejected at the $\alpha = 0.05$ level of significance. The particular statistical realization has an unlikely bimodal distribution that affects the chi-square goodness of fit test at this particular frequency.

Table 8.5.1			
Normalized Errors			
	ϵ_r	ϵ_b	ϵ_{rms}
Characteristic Value	≈ 0.2	≈ 0	≈ 0.2
Maximum Value	0.54	1.9	1.9

Table 8.5.2			
Approximate Number of Degrees of Freedom			
Normalized Frequency	10/512	50/512	200/512
Degrees of Freedom	> 40	≈ 36	> 40

512 MLM estimates of order 32
on 576 points 05-22-88



Mean and Envelope of 512 MLM estimates of order 32
on 576 points 05-22-88

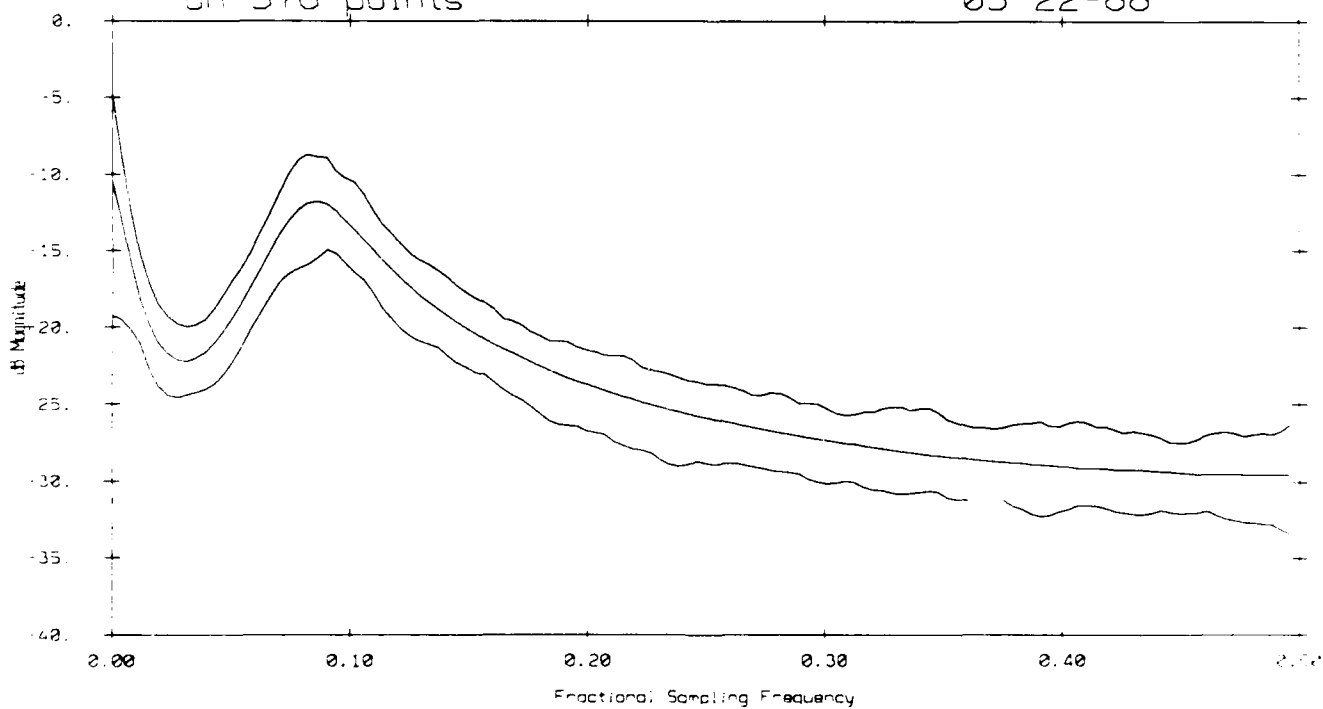


Figure 8.5.1 512 overlaid spectral densities computed by the MLM method on 576 points with an order p of 32

Figure 8.5.2 Mean and envelope of the spectral densities

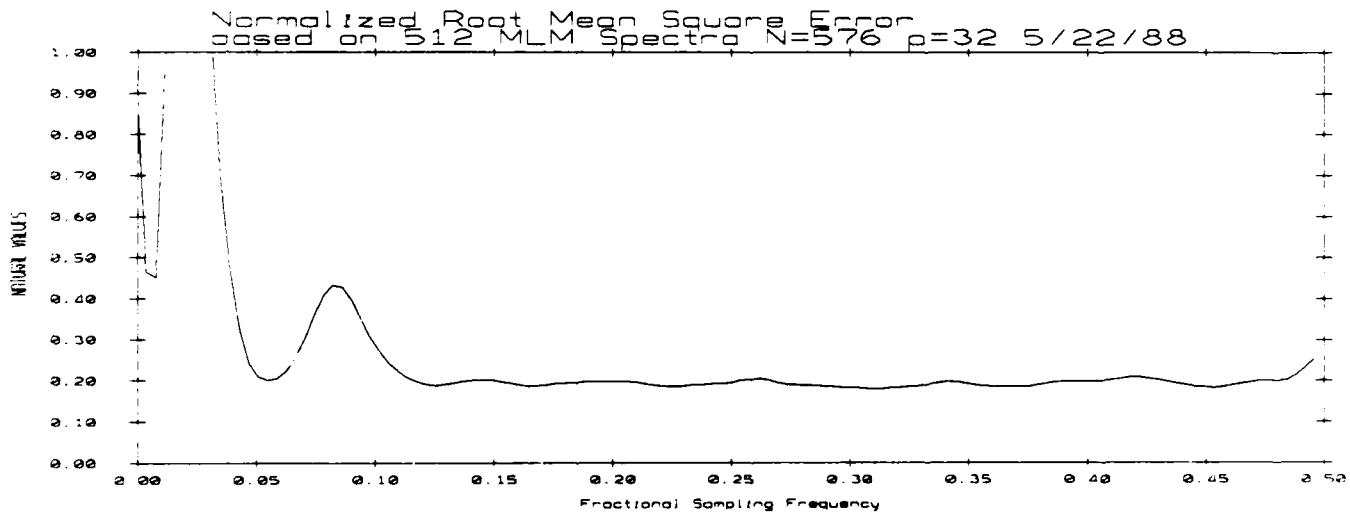
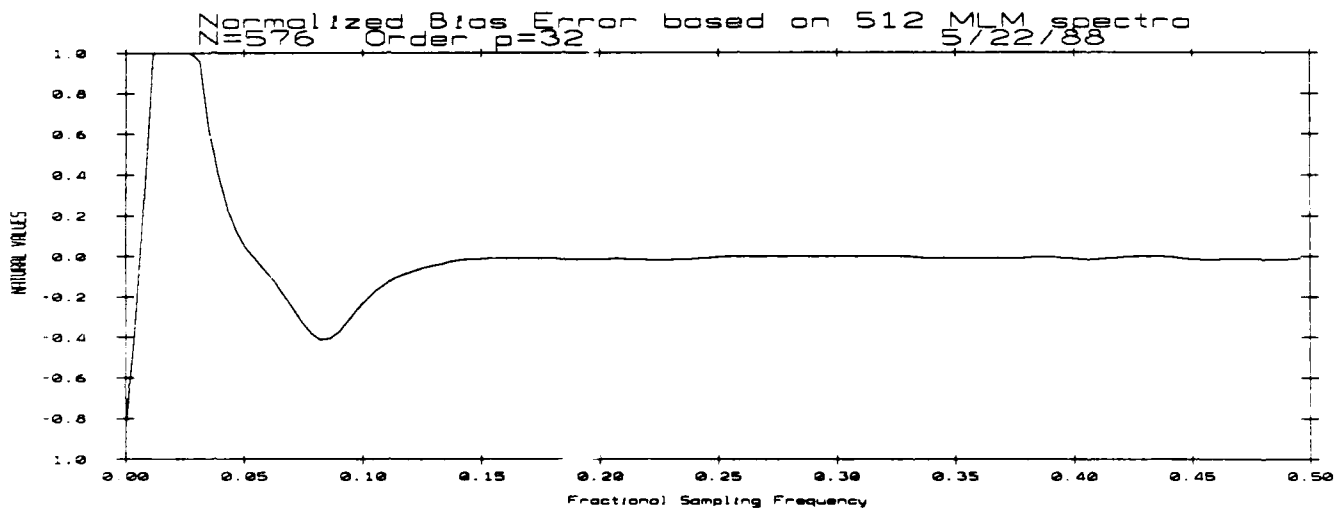
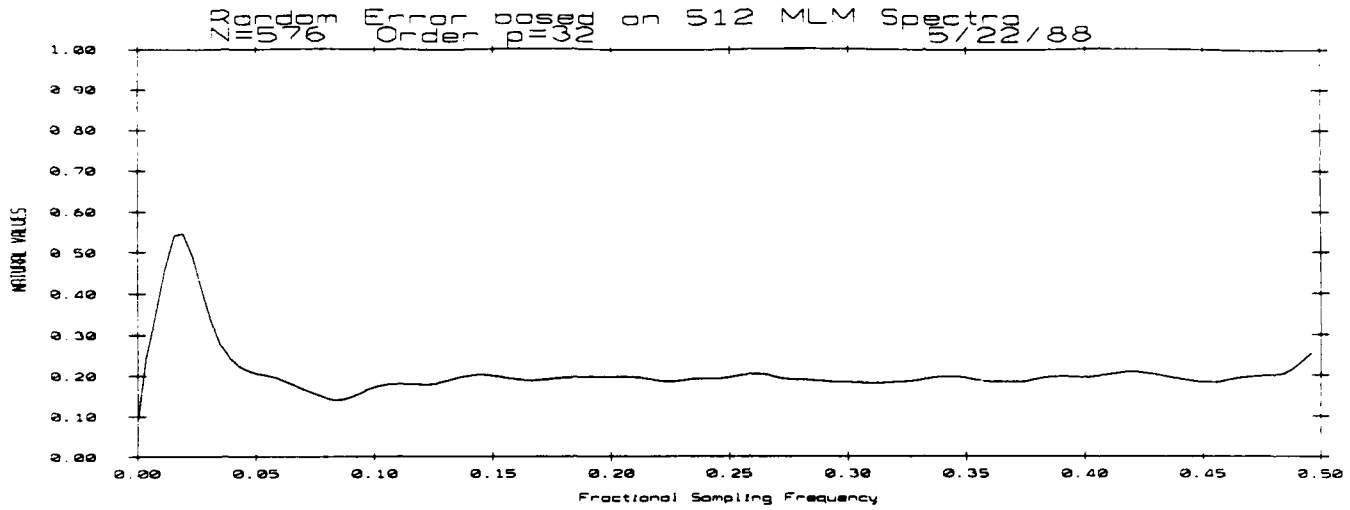


Figure 8.5.3 Normalized random error ϵ_r

Figure 8.5.4 Normalized bias error ϵ_b

Figure 8.5.5 Normalized rms error ϵ_{rms}

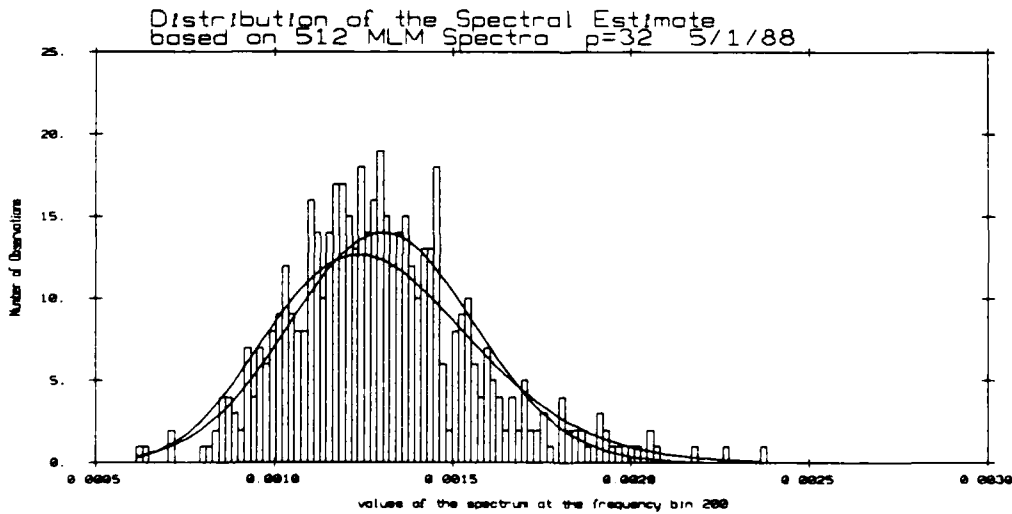
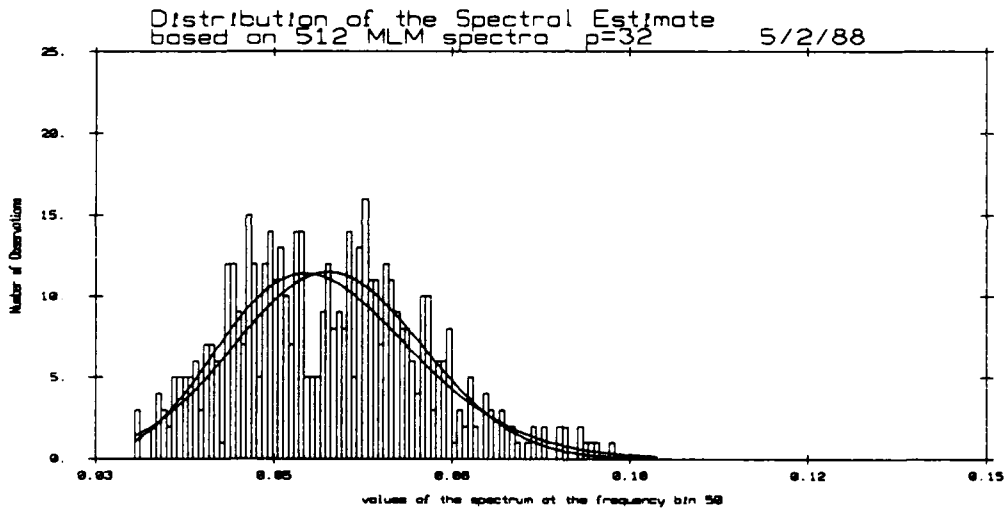
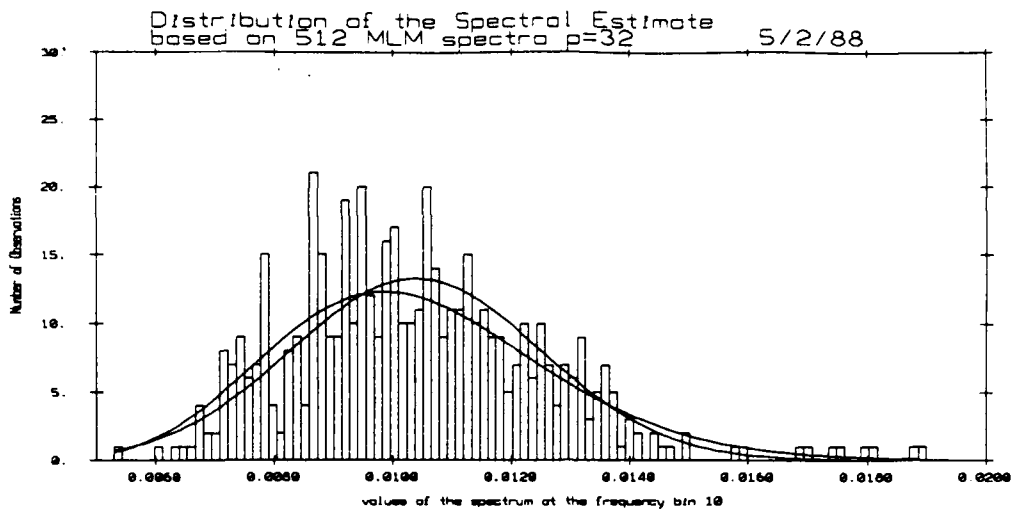


Figure 8.5.6 Sample histogram at the normalized frequency 10/512 overlaid with fitted Gaussian and χ^2_{40} distributions.

Figure 8.5.7 Sample histogram at the normalized frequency 50/512 overlaid with fitted Gaussian and χ^2_{36} distributions.

Figure 8.5.8 Sample histogram at the normalized frequency 200/512 overlaid with fitted Gaussian and χ^2_{40} distributions

9. Conclusions

The results are summarized in terms of the normalized error terms (§2) in Table 9.1, 9.2, 9.3 and in terms of the number of degrees of freedom in Table 9.4. The reference estimator is the conventional FFT method based on 576 points using 8 incoherently averaged FFTs on 128 data points with 50 % overlap and a Hanning window. The tables include a relative efficiency measure defined as the percentage ratio of the rms or random error of the reference estimator (averaged FFTs) to the rms or random error of the particular method [9].

The MLM spectral estimates of order 32 and the MW spectral estimates with a time bandwidth NW of 4, based on the same 576 data sequences, allow a comparison of the three methods for a fixed number of points. In all cases, the underlying spectral density is well resolved. The MLM estimator seems to be the best in this simulation when bias, random and rms errors are considered.

The resolution of the MW method when processing 576 points is given by the Slepian window bandwidth $2W$, in the present case $2W$ is $8/576$ or $1/72$. The resolution of the conventional FFT based method is given by the Hanning window width which is approximately two bins [10] or $2/128$ that is $1/64$. The results given by these two methods are equivalent in term of the normalized errors, with a barely better conventional estimate.

The distributions of the MLM estimates of order 32 and on 576 points are almost Gaussian. On the contrary, the MW and FFT based distributions are almost equivalent chi-squares, although the MW method seems to lose four degrees of freedom at low frequency (in the red and low magnitude part of the power spectral density) with respect to the conventional FFT estimates. This is due to the adaptive weighting of the eigenspectra.

Varying statistical properties with the spectral density shape and dynamic range are also characteristic of the MLM estimators when the number of points in the data sequence is reduced to 128. Such variations are dramatic, given the more stringent conditions. The MW method and the MLM method of order 8 on 128 data points loose statistical consistency at low frequency in the neighborhood of the power spectral density dip near the normalized frequency 0.0625.

In this simulation on short data sequence, the results seem also favorable to the MLM method of order 16 or 32. In addition to good statistical consistency, that is a larger number of degrees of freedom, especially at low frequency, the average rms and random error are lower than the MW method ones. This is especially clear looking at the relative efficiencies with respect to the conventional FFT method.

At high frequency, the rms and random error efficiency of the MLM method, for 128 point long sequence and an order equal to 16 or 32, is above 100% ; this is also the case when the MLM estimates are computed on 576 points. It means that the estimates are better than the conventional FFT estimator. This result is expected since the MLM method can be shown to be equivalent to an average of AR based estimates. Since data were created by an ARMA process, they are well modeled by the MLM method in the high end of the frequency band. The general results are not likely an artifact due to the data since the low frequency end (dip) corresponds to the moving average part of the spectrum. Even at low frequency, the errors are lower and the number of degrees of freedom is higher in the MLM estimates with p equal 16 or 32 than for the MW estimates.

	Average on [0,1/2]	Average on [1/4,1/2]	Maximum value	Value at 10/512	Value at 50/512	Value at 200/512
Conventional FFT method on 576 points, 8 incoherent averaged FFTs on 128 points with a Hanning window	0.42381	0.36612	3.46	0.64180	0.37137	0.38561
	100%	100%		100%	100%	100%
MW method on 576 points with a time bandwidth product of 4 and 8 windows	0.44073	0.40454	4	0.64095	0.35626	0.43107
	94.75%	90.50%		100.13%	104.24%	89.45%
MLM method of order 32 on 576 points	0.28667	0.19512	1.8	1.7516	0.35181	0.19732
	147.82%	187.64%		36.64%	105.56%	195.42%
MW method on 128 data points with a time bandwidth product of 2 and 4 windows	0.99442	0.61816	21.52	9.9947	0.49976	0.59471
	42.6%	59.23%		6.42%	74.31%	64.84%
MW method on 128 data points with a time bandwidth product of 3 and 6 windows	1.2934	0.4881	33.55	30.47	0.4119	0.47612
	32.77%	75%		2.1%	90.16%	80.99%
MLM method of order 8 on 128 data points	1.1073	0.38145	13.6	10.10	0.59446	0.37503
	38.3%	95.98%		6.35%	62.47%	102.82%
MLM method of order 16 on 128 data points	0.63306	0.29789	7	6.002	0.53242	0.2831
	66.95%	122.9%		10.69%	69.75%	136.21%
MLM method of order 32 on 128 data points	0.50334	0.3995	2.5	2.4015	0.54416	0.3897
	84.2%	91.63%		26.72%	68.24%	98.95%

	Average on [0.1/2]	Average on [1/4, 1/2]	Maximum Value	Value at 10/512	Value at 50/512	Value at 200/512
Conventional FFT method on 576 points, 8 incoherent averaged FFTs on 128 points with a Hanning window	0.39652	0.3658	2.1	0.49276	0.37135	0.38556
	100%	100%		100%	100%	100%
MW method on 576 points with a time bandwidth product of 4 and 8 windows	0.41745	0.40171	2.8	0.54777	0.35624	0.42792
	94.98 %	91.06 %		89.95%	104.24	90.10%
MLM method of order 32 on 576 points	0.20537	0.1949	0.54	0.54083	0.15672	0.19730
	193.1%	187.68%		91.11%	236.95%	195.41%
MW method on 128 data points with a time bandwidth product of 2 and 4 windows	0.89055	0.61506	16.9	7.2164	0.49666	0.59317
	44.5%	59.92%		6.83%	74.77%	65%
MW method on 128 data points with a time bandwidth product of 3 and 6 windows	1.6756	0.4481	26	23.394	0.39436	0.47519
	23.66%	75.45%		2.1%	94.16%	81.14%
MLM method of order 8 on 128 data points	0.6578	0.27465	7.5	6.42	0.14386	0.26765
	60.3%	133.2%		7.67%	258.1%	144.05%
MLM method of order 16 on 128 data points	0.42701	0.29731	3.5	3.3134	0.20199	0.28232
	92.86%	123.04%		14.87%	183.85%	136.57%
MLM method of order 32 on 128 data points	0.411	0.3653	1.6	1.5943	0.28698	0.35228
	96.5%	100.12%		30.9%	129.4%	109.44%

	Average on [0.1/2]	Average on [1/4.1/2]	Maximum Value	Value at 10/512	Value at 50/512	Value at 200/512
Conventional FFT method on 576 points, 8 incoherent averaged FFTs on 128 points with a Hanning window	0.05818	0.00459	2.75	0.4112	-0.0043	0.0063
MW method on 576 points with a time bandwidth product of 4 and 8 windows	0.07655	0.04548	2.8	0.33282	-0.0039	0.0519
MLM method of order 32 on 576 points	0.03479	-0.0044	1.9	1.6661	-0.31498	-0.0029
MW method on 128 data points with a time bandwidth product of 2 and 4 windows	0.3187	0.05583	13.26	6.9151	-0.0556	0.04267
MW method on 128 data points with a time bandwidth product of 3 and 6 windows	0.59163	0.05236	21.2	19.525	-0.1218	0.02971
MLM method of order 8 on 128 data points	0.2636	0.2636	11	7.7991	-0.5767	0.2627
MLM method of order 16 on 128 data points	0.2139	-0.01623	6.2	5.005	-0.4926	-0.0211
MLM method of order 32 on 128 data points	-0.0964	-0.16083	2	1.7959	-0.46233	-0.1666

	Frequency 10/512	Frequency 50/512	Frequency 200/512
Conventional FFT method on 576 points, 8 incoherent averaged FFTs on 128 points with a Hanning window	16	16	14
MW method on 576 points with a time bandwidth product of 4 and 8 windows	12	16	14
MLM method of order 32 on 576 points	> 40	≈ 36	> 40
MW method on 128 data points with a time bandwidth product of 2 and 4 windows	< 2	8	6
MW method on 128 data points with a time bandwidth product of 3 and 6 windows	< 2	10	10
MLM method of order 8 on 128 data points	< 2	16	36
MLM method of order 16 on 128 data points	6	12	20
MLM method of order 32 on 128 data points	6	6	10

10. References

- [1] D.J. Thomson, "Spectrum Estimation and Harmonic Analysis", Proceedings of the IEEE, Vol 70, No. 9, pp 1055-1096, September 1982.
- [2] A.D. Chave, "Notes on Spectral Analysis", Lecture Notes, 11 pages.
- [3] A.D. Chave, "Multiple Window Spectrum Analysis", Lecture Notes, 13 pages, January 1988.
- [4] R.J. Urick, "Ambient Noise In The Sea", Peninsula Eds, 1984.
- [5] J.S. Bendat, A.G. Piersol, "Random Data, Analysis and Measurement Procedures", John Wiley Eds, Second Edition, 1986.
- [6] R.T. Lacoss, "Data Adaptive Spectral Analysis Methods", Geophys., vol 36, pp 661-675, August 1971.
- [7] S.L. Marple, "Digital Spectral Analysis", Prentice Hall Eds, 1987.
- [8] S.M. Kay, "Modern Spectral Estimation : Theory and Application", Prentice Hall Eds, 1988.
- [9] M.B. Priestley, "Spectral Analysis and Time Series", Vol 1, Academic Eds, 1981.
- [10] F.J. Harris , "On The Use Of Windows For Harmonic Analysis With The Discrete Fourier Transform", Proceedings of the IEEE, Vol 66, No. 1, pp 51-83, January 1978.

REPORT DOCUMENTATION PAGE

1a. REPORT SECURITY CLASSIFICATION UNCLASSIFIED		1b. RESTRICTIVE MARKINGS	
2a. SECURITY CLASSIFICATION AUTHORITY		3. DISTRIBUTION / AVAILABILITY OF REPORT Approved for public release; distribution unlimited.	
2b. DECLASSIFICATION / DOWNGRADING SCHEDULE			
4. PERFORMING ORGANIZATION REPORT NUMBER(S) MPL Technical Memorandum 403 [MPL-U-16/88]		5. MONITORING ORGANIZATION REPORT NUMBER(S)	
6a. NAME OF PERFORMING ORGANIZATION Marine Physical Laboratory	6b. OFFICE SYMBOL (if applicable) MPL	7a. NAME OF MONITORING ORGANIZATION Office of Naval Research Department of the Navy	
6c. ADDRESS (City, State, and ZIP Code) University of California, San Diego Scripps Institution of Oceanography San Diego, CA 92152		7b. ADDRESS (City, State, and ZIP Code) 800 North Quincy Street Arlington, VA 22217-5000	
8a. NAME OF FUNDING / SPONSORING ORGANIZATION Office of Naval Research	8b. OFFICE SYMBOL (if applicable) ONR	9. PROCUREMENT INSTRUMENT IDENTIFICATION NUMBER N00014-87-C-0127	
8c. ADDRESS (City, State, and ZIP Code) Department of the Navy 800 North Quincy Street Arlington, VA 22217-5000		10. SOURCE OF FUNDING NUMBERS	
		PROGRAM ELEMENT NO.	PROJECT NO.
		TASK NO.	WORK UNIT ACCESSION NO.
11. TITLE (Include Security Classification) Broadband Spectral Estimation Using the Multiple Window Method: A Comparison with Classical Techniques			
12. PERSONAL AUTHOR(S) Jean-Marie Tran			
13a. TYPE OF REPORT Summary	13b. TIME COVERED FROM _____ TO _____	14. DATE OF REPORT (Year, Month, Day) June 1988	15. PAGE COUNT 48 pgs
16. SUPPLEMENTARY NOTATION			
17. COSATI CODES		18. SUBJECT TERMS (Continue on reverse if necessary and identify by block number)	
FIELD	GROUP	spectral estimation, Discrete Fourier Transform, data adaptive weighting, acoustic ambient noise	
19. ABSTRACT The Multiple Window recently introduced by D.J. Thomson is an alternative approach to spectral estimation. Using an orthogonal decomposition of the Discrete Fourier Transform of the data on the prolate spheroidal wave sequences, the power spectrum is estimated by a weighted average of raw spectra obtained from the Fourier transforms of the data windowed by the prolate sequences. This method has the reputation of working well on short data sequences, offering good variance control and a fair resolution. Because the Multiple Window technique combines Fourier transforms with data adaptive weighting, it is compared, in a Monte Carlo simulation, to more conventional spectral estimation methods: the classic averaged Fourier transforms technique and Capon's Maximum Likelihood method. The underlying spectral density to be estimated is of an ARMA process simulating underwater acoustic ambient noise. It is characterized by a moderate dynamic range of 30 dB and can be regarded as a generic spectrum of many applications. The three methods considered here are non parametric, so that no estimator has an unfair advantage. The normalized bias, random and root mean square errors, as well as the statistical distributions, based on 512 realizations of the spectral density, quantify the performance of the three different techniques.			
20. DISTRIBUTION / AVAILABILITY OF ABSTRACT <input type="checkbox"/> UNCLASSIFIED/UNLIMITED <input checked="" type="checkbox"/> SAME AS RPT <input type="checkbox"/> DTIC USERS		21. ABSTRACT SECURITY CLASSIFICATION UNCLASSIFIED	
22a. NAME OF RESPONSIBLE INDIVIDUAL W. S. Hodgkiss		22b. TELEPHONE (Include Area Code) (619) 534-1798	22c. OFFICE SYMBOL MPL